INFORMATION TO USERS

This manuscript has been reproduced from the microfilm master. UMI films the text directly from the original or copy submitted. Thus, some thesis and dissertation copies are in typewriter face, while others may be from any type of computer printer.

The quality of this reproduction is dependent upon the quality of the copy submitted. Broken or indistinct print, colored or poor quality illustrations and photographs, print bleedthrough, substandard margins, and improper alignment can adversely affect reproduction.

In the unlikely event that the author did not send UMI a complete manuscript and there are missing pages, these will be noted. Also, if unauthorized copyright material had to be removed, a note will indicate the deletion.

Oversize materials (e.g., maps, drawings, charts) are reproduced by sectioning the original, beginning at the upper left-hand corner and continuing from left to right in equal sections with small overlaps. Each original is also photographed in one exposure and is included in reduced form at the back of the book.

Photographs included in the original manuscript have been reproduced xerographically in this copy. Higher quality 6" x 9" black and white photographic prints are available for any photographs or illustrations appearing in this copy for an additional charge. Contact UMI directly to order.

UMI

A Bell & Howell Information Company
300 North Zeeb Road, Ann Arbor MI 48106-1346 USA
313/761-4700 800/521-0600

Université d'Ottawa · University of Ottawa

Alternative Splicing and Genomic Organization of the SLAP gene encoding Sarcolemmal-Associated Proteins.

by

Paul A. Wielowieyski

Department of Pharmacology
Faculty of Medicine
University of Ottawa
Ottawa, Ontario, Canada

A thesis submitted to the School of Graduate Studies and Research
in conformity with the requirements for the
degree of Master of Science.

ABSTRACT

Sarcolemmal-associated proteins (SLAPs) are a family of acidic amphipathic alpha-helical proteins associated with the membrane. Different size SLAP transcripts were identified and shown to encode polypeptides of 37, 46 and 74 kDa designated by SLAP1, SLAP2 and SLAP3, respectively. The SLAP1 and SLAP2 transcripts were expressed in cardiac, soleus and smooth muscle, whereas SLAP3 was expressed ubiquitously. The subcellular distribution studies localized SLAPs to cell membrane, as well as sarco/endoplasmic reticulum membrane and transverse-tubules. The SLAP family is encoded by a single gene which was mapped to a human chromosome 3p14.3-21.2 and the various transcripts are perhaps generated by alternative promoter and/or alternative splicing.

In order to understand the molecular basis underlying the SLAP isoform diversity studies were carried out to elucidate the genomic organization of the SLAP gene. The 3' end of SLAP gene is composed of 11 exons spanning over 35 kb, that range in size from 60 to 321 bp. SLAP introns on the other hand, range in size from 0.2 to 5.5 kb and all conform to a canonical GT-AG rule.

Results suggest that SLAP primary transcript is alternatively spliced and that the expression of alternative variants is regulated in a developmental and tissue specific manner. Moreover, RT-PCR and cDNA library screening isolated alternatively spliced human, rabbit and rat orthologues that have been evolutionarily conserved which is indicative of a functional role of the various variants. Although the function of various SLAP variants remains unknown the alternative

splicing is predicted to introduce putative phosphorylation sites, influence secondary structure and perhaps alter subcellular localization.

In summary, heterogeneity due to alternative usage of the N-terminal of SLAP combined with the diversity generated by alternative splicing is predicted to give rise to 36 distinct SLAP isoforms, that may perhaps play distinct roles in the membrane function.

ACKNOWLEDGMENTS

I would like to express my appreciation to my thesis supervisor Dr. Balwant S. Tuana for his support and encouragement throughout my graduate program.

A special thanks to Maysoon Salih for providing me with technical experience and assistance, as well as Rosa Guzzo, John Leddy, M. Serdal Sevinc, Shereeni Veerasingham and Jeffrey Wigle.

My deepest gratitude to my family, friends and Dear Natalie for ongoing support, encouragement and patience throughout the course of this work.

Dedicated to my Parents

and Dear Natalie

TABLE OF CONTENTS

MATERIALS AND METHODS

LIST OF FIGURES

LIST OF TABLES

DIRECTORY OF ABBREVIATIONS

Amp	Ampicillin
AP	Action Potential
AV	Anterioventricular
ATP	Adenosine 5'-triphosphate
cDNA	Complementary DNA
dATP	Deoxyadenosine 5'-triphosphate
dCTP	Deoxycytosine 5'-triphosphate
ddNTP	Dideoxynucleoside 5'-triphosphate
Ca^{2+}	Calcium ion
CAM-kinase	Calmodulin-dependent kinase
CICR	Ca^{2+}-induced Ca^{2+} release
DEPC	Diethylpyrocarbonate
DHP	1,4-Dihydropyridine
DNA	Deoxyribonucleic acid
DNase	Deoxyribonuclease
DTT	Dithiotreitol
EDTA	Ethylenediaminetetraacetic acid
EtOH	Ethanol
EtBR	Ethydium bromide
IPTG	beta-D-Isopropyl-thiogalactopyranosine
HCl	Hydrochloric acid

kb	Kilobase
kDa	KiloDaltons
LB broth	Luria-Bertani medium containing bacto-tryptone, bacto-yeast extract and NaCl
mRNA	Messenger RNA
MW	Molecular weight
min	Minutes
NaOAc	Sodium Acetate
NCX	Na^+-Ca^{2+} exchanger
NZCYM	Medium containing NZ amine, bacto-yeast extract, NaCl, and $MgSO_4$
PEG 8000	Polyethyene glycol (MW 8000)
PEG hyb solution	hybridization solution containing PEG, SDS and SSPE
pfu	Plaque forming units
PLB	Phospholamban
PKA	cAMP-dependent protein kinase
PKC	protein C kinase
PKG	cGMP-dependent kinase
PMCA	Plasma membrane Ca^{2+}-ATPase
RNA	Ribonucleic acid
RNase	Ribonuclease
rpm	revolutions per minute
RYR	Ryanodine

SA	Sinoatrial
SDS	Sodium dodecyl sulfate
sec	Seconds
SERCA	Sarco-endoplasmic reticulum Ca^{2+}-ATPase
SLAP	Sarcolemma Associated Protein
SM	Suspension medium containing 100 mM NaCl, 50 mM Tris-HCl, $MgSO_4$ and 0.01% gelatin
SR	Sarcoplasmic Reticulum
SSC	Buffer containing 150 mM NaCl and 15 mM sodium citrate (pH 7.0)
SSPE	Buffer containing 150 mM NaCl, 10 mM $NaH_2PO_4.H_2O$ and 1 mM EDTA pH 7.4
TAE	Tris-Acetate Buffer containing 40 mM Tris-Acetate and 1 mM EDTA (pH 8.0)
TBE	Tris Buffer containing 89 mM Tris-Borate, 89 mM boric acid and 2 mM EDTA (pH 8.0)
TE buffer	Tris buffer containing 1 mM EDTA pH 8.0
TriPure	Monophasic solution of phenol thiocyanate
X-gal	5-bromo-4-chloro-3-indoyl-B galactoside dissolved in dimethyl formamide
ul	Microliter
UV	Ultra-violet

INTRODUCTION

A family of putative Ca^{2+} binding proteins referred to as SLAPs (sarcolemmal-associated proteins) was shown to be highly expressed in cardiac membrane systems. In view of the importance of Ca^{2+}-binding proteins in regulation of the cardiac function, studies were carried out to elucidate the genomic organization and to investigate alternative splicing of SLAP. The introduction describes the importance of Ca^{2+}-binding proteins in Ca^{2+} homeostasis in cardiac function. The introduction also describes the background information on the SLAP protein and their potential role in cardiac function and Ca^{2+} regulation.

1.1. Myocardium

The heart is a complex organ dedicated to the pumping of blood. Contractility of the heart is attributed to concerted shortening of its contractile units, the cardiomyocytes. Contraction is a result of the cross-bridge cycling of actin and myosin filaments. Cardiac contractility is initiated by spontaneous depolarizations of pacemaker cells located in the sinoatrial (SA) and anterioventicular (AV) nodes, that initiate the action potentials (APs). Conductive cells of the heart are responsible for propagation of APs from the SA node to the AV node and subsequently to all the parts of the heart. The AP-induced depolarizations of cardiomyocyte cell membrane result in an increase of intracellular Ca^{2+} which signals muscle contractions.

1.2. Ultrastructure of Contractile Cells.

The myocardial cell is enclosed by sarcolemma which establishes a barrier between the extracellular and intracellular environments. The sarcolemma periodically invaginates to form an extensive tubular network, known as T-tubules, extending the extracellular environment into the interior of the myocyte. Sarcolemma and T-tubules contain ion pumps that establish Ca^{2+}, Na^{+} and K^{+} ion gradients, as well as ion channels pertinent to corresponding ion fluxes.

The myocardial cells contain large numbers of contractile proteins that are organized into myofibrils. Myofibrils are composed of arrays of elementary contractile units, the sarcomeres, that provide machinery for contraction. The cross-bridge cycling associations of the thick (myosin) and thin filaments (actin) of sarcomere result in sliding of the interdigitating filaments causing sarcomere shortening and thus resulting in muscle contraction (Huxley 1957).

The sarcoplasmic reticulum (SR) is a specialized Ca^{2+} store that forms an extensive intracellular membrane system. The SR is both structurally and functionally divided into two regions: the subsarcolemmal cisternae, which contain Ca^{2+} release channels, and an extensive sarcotubular network that contains Ca^{2+} pumps. The SR Ca^{2+} release channels and Ca^{2+} pumps represent the functional components responsible for Ca^{2+} exchange during contraction-relaxation cycling. In the heart myocyte, subsarcolemmal cisternae are located both beneath the sarcolemma and alongside the T-tubule system, whereas the sarcotubular network surrounds the contractile proteins in the center of the sarcomere (Lytton 1992).

Interspersed among the myofibrils and in subsarcolemmal regions are mitochondria

which principally generate energy in the form of ATP needed to maintain cardiac contractility and associated ion gradients. Although mitochondria can accumulate large amounts of Ca^{2+} (Carafoli 1985), they do not contribute its Ca^{2+} pool to the Ca^{2+} mobilization occurring during cardiac contraction. Instead, mitochondrial Ca^{2+} stores are thought to play a protective role in Ca^{2+} overload in pathological states (Carafoli 1987).

1.3. Excitation-Contraction Coupling.

Excitation-contraction (E-C) coupling is a term describing the coupling of an electrical impulse on the sarcolemmal membrane with the increase in intracellular Ca^{2+} concentration from 10^{-7} to 10^{-5} M leading to muscle contraction (Franzini-Armstrong 1994). In skeletal and cardiac muscle E-C coupling operates by fundamentally different mechanisms. In cardiac E-C coupling, the entry of trans-sarcolemmal Ca^{2+} into the cell is required to produce further Ca^{2+}-induced Ca^{2+}-release (CICR) from the SR (Fabiato 1983). Although Ca^{2+} entry through the voltage-gated channel in T-tubules is believed to deliver the trans-sarcolemmal "trigger" Ca^{2+} (Catterall 1991), there is mounting evidence that the Na^{+}-Ca^{2+} exchanger (NCX) could also contribute to the "trigger" Ca^{2+} (Leblanc 1990, Kohomoto 1994 and Litwin 1996).

The dependence of cardiac CICR on trans-sarcolemmal "trigger" Ca^{2+} is strongly supported by experiments in which addition of cadmium or removal of extracellular calcium abolishes all contractions (Ebashi 1976), as well as the molecular characterization of a Ca^{2+} release channel on the SR in anatomical proximity to the sarcolemmal T-tubule (Berridge 1993 and Flucher 1996).

In skeletal muscle, trans-sarcolemmal Ca^{2+} entry is not required for E-C coupling, but rather is believed to be due to electrical depolarization or mechanical coupling of voltage sensor (L-type Ca^{2+} channels) on sarcolemma and T-tubules to the Ca^{2+} release channels on SR (Caswell 1989, Rios 1991 and Catterall 1991).

1.4. Ca^{2+} Homeostasis in E-C coupling.

Contraction-relaxation cycling of the heart muscle is controlled by free cytosolic Ca^{2+} concentration, which is regulated by two membrane systems, sarcolemma/T-tubules and SR (Fleischer 1989). Following the depolarization of the sarcolemma/T-tubules extracellular Ca^{2+} enters the myocyte via L-type voltage-dependent Ca^{2+} channels. The entering "trigger" Ca^{2+} induces a much greater recruitment of Ca^{2+} from intracellular SR stores (Fabiato 1985). The Ca^{2+} mobilized during E-C coupling is localized to sarcolemma and lumen of the SR. The sarcolemmal pool is attributed to Ca^{2+} binding to negatively charged sarcolemmal phospholipids (Philipson 1980 and Langer 1983) and several sarcolemmal proteins including: Ca^{2+} channels, Na^{+}-Ca^{2+} exchanger, and 125 and 97 kDa glycoproteins (Tuana 1991). The sarcolemmal Ca^{2+} pool represents a source of the "trigger" trans-sarcolemmal Ca^{2+} which, however, is insufficient to activate the contractile apparatus. The SR Ca^{2+} pool, on the other hand, contributes a much larger amount of Ca^{2+} that increases $[Ca^{2+}]_i$ to the micromolar range sufficient for induction of cardiac contraction. The SR Ca^{2+} system is also involved in an active sequestration and storage of Ca^{2+} and plays a major role in muscle relaxation (Lytton 1992).

The CICR from the SR pool results in Ca^{2+} binding to troponin-C, the Ca^{2+} receptor of the contractile proteins. Subsequently troponin-C undergoes a conformational transition, that is further transmitted to other components of the troponin complex; (troponin-I, troponin-T and tropomyosin), resulting in disinhibition of actin-myosin interaction (Tobacman 1996).

An increase of $[Ca^{2+}]_i$ also activates another cellular Ca^{2+} sensor, calmodulin, that exerts multiple regulatory functions on numerous physiological processes of cardiac muscle. These include energy and biosynthetic metabolism, cytoskeletal assembly and intracellular modulation of other second messengers such as cAMP and Ca^{2+} concentration (Vogel 1994).

Following each E-C coupling cycle cytoplasmic Ca^{2+} has to be lowered to resting levels in order to attain relaxation. This is accomplished primarily by the Ca^{2+} pump of SR and the sarcolemmal Na^{+}-Ca^{2+} exchanger, and to a smaller extent by the plasma membrane Ca^{2+} ATPase (PMCA).

1.5. Molecular basis of E-C coupling.

The sarcolemma plays a critical role in control of E-C coupling by providing the "trigger" Ca^{2+}. It is also responsible for regulation of Ca^{2+}, Na^{+} and K^{+} ion fluxes during depolarization-repolarization, acid-base homeostasis and cell volume. The control of ion fluxes is carried out by ion channels and ion transporters embedded within the lipid bilayer. The ion channels operate as gating mechanisms allowing the movement of ions along their corresponding gradients, while ion transporters restore the resting state.

Voltage-dependent ion channels of sarcolemma are involved in depolarization and repolarization of cardiac cells during the cardiac contraction-relaxation cycle. The electrical impulse causing depolarization of sarcolemma consists of three phases. The initial phase is mediated by activation of voltage-dependent Na^+ channels causing a rapid depolarization of the sarcolemma. The second phase or plateau is maintained by long-lasting opening of the L-type Ca^{2+} channels. The terminal phase occurs upon activation of K^+ outward channels and results in repolarization of the sarcolemma (Catterall 1988).

Cloning of the voltage-dependent ion channels revealed a significant homology in the primary structure, particularly in the transmembrane hydrophobic segments and an overall ion channel topology. The striking molecular similarities and the structural conservation among voltage-dependent ion channels suggest a divergent evolution from a common ancestral protein (Catterall 1988 and Schwartz 1989). The K^+-, Na^+- and Ca^{2+}-channels contain a major alpha-subunit, that forms an ion pore, composed of four transmembrane repeats with each repeat consisting of six transmembrane helices. Unlike Na^+- and Ca^{2+}-channels which are composed of four homologous repeats, K^+-channel is composed of four identical subunits (Jan 1989). A 'pore' segment and a voltage sensor both represent conserved features of the voltage-gated ion channels. P-segment localized to the loop between S5 and S6 is responsible for the pore formation and ion selectivity, whereas the voltage sensor, in the transmembrane segment S4, activates the voltage-dependent channels in response to a change in membrane potential (Catterall 1993).

a) Ca^{2+} Influx via Voltage-dependent Ca^{2+} Channels.

Cardiac tissue contains two types of voltage- and time-dependent Ca^{2+} channels displaying L-type (long-lasting) and T-type (transient) conductances (Bean 1985).

The **L-type** Ca^{2+} channels are more predominant in the myocardium and are primarily located in T-tubules. They provide the "trigger" Ca^{2+} for the cardiac CICR, that contributes to the plateau phase of depolarization and regulates the extent of Ca^{2+} release from SR during excitation-contraction coupling (Bouchard 1995). The cardiac L-type Ca^{2+} channels exhibit high-voltage-activated (-40 to -30 mV) and slow inward-long-lasting current (25 pS) (Kostyuk 1989). Their conductance is blocked by three different classes of pharmacological agents: the benzothiazepines (eg. diltiazem), the dihydropyridines (eg. nifedipine) and the phenylalkylamines (eg. verapamil).

The L-type Ca^{2+} channels of non-muscle excitable cells, are involved in excitation-secretion (endocrine cells and some neurons) (Catterall 1988). The L-type Ca^{2+} channels are encoded by three distinct genes: S, C and D according to nomenclature introduced by Snutch *et al.* in 1992. The cardiac L-type channels is encoded by class C gene, although possible expression of class D gene has not been excluded. The C and D genes are mapped to human chromosomes 12p13.3 and 3p14.3, respectively.

The function of the **T-type** channel is still unknown, however, due to its low activation threshold and its high expression in sinusal cells, it is postulated to play a role in pacemaker activity (Vassort 1994).

Other voltage-dependent Ca^{2+} currents have been identified including N-type, P-type, Q-type and R-type, however, they are not expressed in the heart (Tsien 1991).

The **cardiac L-type channels** are multisubunit structures, analogous in subunit composition to skeletal L-type channels, formed by association of alpha1, alpha2-delta and beta subunits (Tuana 1990). The alpha1 subunit encodes a functional ion pore composed of well conserved voltage-dependent channel topology. The utilization of structure-function studies of cardiac and skeletal isoforms allowed to allocate well characterized biological and pharmacological properties to specific regions of the alpha1 subunit. The role of cardiac and skeletal alpha1 subunits in E-C coupling was established using the mouse dysgenic model (mdg) (Tanabe 1988 and 1990a) with the second intracellular loop (between repeats II and III) as its critical determinant (Tanabe 1990b). The pore of the channel is confined to a loop between segments 5 and 6 (SS1-SS2), called P-loop, of each domain (Sather 1994). Ion selectivity is allocated to glutamates of the P-loop because non-conservative mutagenesis of critical glutamates for Arg\Lys results in an altered permeability from Ca^{2+} to Na^{+} while the conservation of DHP sensitivity is maintained (Sather 1994). The activation domain of the L-type channel is located to S3 segment and S3-S4 linker of repeat I (Nakai 1993), whereas S6 segment of repeat I and N-terminal of the first intracellular loop, corresponded to the inactivation region. The voltage sensor, a conserved feature of voltage-gated channels, is confined to the S4 segment of each of the repeats. Lastly, the DHP binding site is localized to the SS1-SS2 segment of domain IV lining the pore and part of S6. (Catterall 1992 and Varadi 1995).

The functional diversity of cardiac L-type channels is generated by alternative splicing of the C class gene (Diebold 1992, Soldatov 1992, 1995 and 1997) and via heterologous associations with auxiliary subunits (alpha2-delta and beta) (Castellano 1994).

b) Sarcolemmal Ca^{2+} Efflux Systems.

To balance the small amount of "trigger" Ca^{2+} entering the heart cell during each depolarization, an equal amount of Ca^{2+} has to be removed. This is accomplished by two mechanisms: primarily by the NCX and to a smaller extent by the PMCA (Bers 1993).

Similarly, the Na^+ and K^+ ion gradients must also be restored to recover the resting membrane potential and maintain tissue excitability. The Na^+-K^+ ATPase, is responsible for maintenance of low Na^+ and high K^+ concentration in the intracellular milieu, which is crucial for the preservation of the membrane potential of all cells, but particularly excitable cells of muscle and brain.

The cardiac **sarcolemmal NCX** is a low affinity, high capacity Ca^{2+} export system that is responsible for removal of Ca^{2+} during relaxation. NCX is an electrogenic anti-port transporter of Na^+ and Ca^{2+} with a stoichiometry of 3:1, that is driven by the energy of the Na^+ gradient established by the Na^+-K^+ ATPase. Molecular cloning revealed that NCX is encoded by a single gene (Nicoll 1990), that via alternative splicing could theoretically generate up to 32 isoforms (Kofuji 1994). The secondary structure of NCX gene predicts 12 transmembrane segments (M1-M12) and a large cytoplasmic loop (between M6-M7) (Nicoll 1990). The loop has an inhibitory effect on the activity of the exchanger, and hence is referred to as an endogenous exchanger inhibitory peptide (XIP) (Matsuoka 1997). The exchanger function is modulated by phosphorylation by a CAM kinase and PKA (Caroni 1983), perhaps in the large intracellular loop containing putative CAM kinase and PKA phosphorylation sites.

In addition to its established role in Ca^{2+} export in relaxation, the NCX was shown

to import Ca^{2+} under specific conditions and thus contribute to "trigger" Ca^{2+}. Normally, direction of electrogenic Na^{+}-Ca^{2+} exchange is responsive to Na^{+} and Ca^{2+} concentrations on either side of the sarcolemma. The model by Leblanc *et al.* predicts that during depolarization (due to opening of the Na^{+} channels) the inner side of the sarcolemma may become positive and perhaps inhibit the entrance of positively charged Na^{+} ions via the exchanger. Thus, the Na^{+} ions that just entered during the opening of the Na^{+}-channels would leave via the exchanger operating in "reverse mode" and Ca^{2+} would enter the cell (Leblanc 1990). Although the physiological significance of Ca^{2+} entering the cell via NCX working in the "reverse mode" remains controversial, several studies have shown that it is sufficient to trigger cardiac CICR (Levesque 1991, Levi 1993 and Mitcheson 1997) in absence of L-type current ($I_{Ca,L}$) and may, therefore, be significant in the normal control of cardiac muscle contraction.

The **PMCA** pump represents another mechanism responsible for the removal of Ca^{2+}, however its rate is much slower than either that of sarcoplasmic NCX or SR SERCA pump. In contrast to NCX, PMCA is a high affinity low capacity system responsible for fine tuning of the intracellular Ca^{2+} concentration. The Ca^{2+} export by PMCA is driven by energy utilized from ATP hydrolysis. However, unlike other Ca^{2+}-ATPases PMCA Ca^{2+}-ATP stoichiometry is 1.0 as opposed to 2.0 observed for the SERCA Ca^{2+} pump (Carafoli 1992).

The PMCA pump exhibits a number of isoforms that are encoded by a multigene family. To date four human PMCA genes have been identified: PMCA 1 (Verma 1988), PMCA 2 (Heim 1992), PMCA 3 (Brown 1996) and PMCA 4 (Strehler 1990) along with

their chromosomal location. Heart expresses two ubiquitous "house keeping" pumps PMCA 1 and PMCA 4 (Stauffer 1993), and PMCA 2 (Brandt 1992).

The secondary structure of the PMCA pump predicts 10 transmembrane segment and 3 large cytoplasmic domains. The long cytoplasmic C-terminal, containing the calmodulin binding domain, acts as an internal restrainer of the pump. Calmodulin binding removes the restraint and facilitates Ca^{2+} transport (Carafoli 1992).

The PMCA pump function is controlled by multiple regulatory mechanisms involving activating interaction with the C-terminal. PMCA is activated by: calmodulin (Tuana 1981), protein kinases: PKA (Caroni 1981), PKC (Wang 1991) and PKG (Yoshida 1991), oligomerization (Kosk-Koscicka 1988 and Vorherr 1991); and controlled proteolysis by calpain (Au 1986, Carafoli 1987 and Wang 1988).

c) Ca^{2+} Fluxes Across Sarcoplasmic Reticulum.

Up to this point the discussion of E-C coupling focused on the sarcolemma containing a complex of ion transport mechanisms that together orchestrate the flow of "trigger" Ca^{2+} and other ions. However, most of the Ca^{2+} that binds troponin-C is derived from the SR, an intracellular Ca^{2+} storage. The Ca^{2+} release channels of SR are activated in response to influx of "trigger" Ca^{2+} across the sarcolemma and thus amplify the "trigger" signal by releasing 10-65 X more Ca^{2+} to activate cardiac contraction (Wier 1994 and Cannell 1995). The SR is also involved in an active removal of intracellular Ca^{2+} by SERCA and Ca^{2+} sequestration via binding to specialized high capacity storage proteins.

The biochemical analysis of isolated SR fractions as well as immunological studies demonstrated the presence of **Ca^{2+} release channels**, **Ca^{2+} pumps** and **Ca^{2+} binding proteins** in subsarcolemmal cisternae, sarcotubular SR and SR lumen, respectively.

The **Ca^{2+} release channels** of SR, also known as ryanodine receptors, are responsible for mobilization of Ca^{2+} from SR stores. The Ca^{2+} release channels form a tetrameric structure, composed of four subunits each of which consists of a large cytoplasmic domain and a transmembranous domain, that transverses the membrane of subsarcolemmal cistern (Saito 1988). The cytoplasmic portions of the Ca^{2+} release channel project as "feet" between the subsarcolemmal cisternae and the T-tubules containing the clusters of voltage-gated L-type Ca^{2+} channels (Stern 1992), thus forming microscopic couplings. It is believed that such clusters are functionally independent of each other (Stern 1992) and are under a 'local control' of "trigger" Ca^{2+} supplied by closely associated L-type channels (Stern 1992, Cannell 1994). The facet of subsarcolemmal cistern directly opposing the T-tubule is highly enriched in ryanodine receptors with nearly 800 receptors per um^2 (Wibo 1991).

Elucidation of the primary structure revealed that each subunit of the tetrameric "foot" protein has a molecular weight of 565 kDa (Takeshima 1989) composed of a massive cytoplasmic domain and four membrane-spanning domains (Wagenknecht 1989 and Takeshima 1989). Recent studies reveal that the majority of the ryanodine receptor structure forms a porous multidomain cytoplasmic assembly that perhaps communicates with its transmembrane region, thus activating the channel opening (Wagenknecht 1997).

At least 3 genes code for the SR Ca^{2+} release channels. RYR1 gene localized on

human chromosome 19q13.1 (MacKenzie 1990) is expressed almost exclusively in skeletal muscle, where it is of critical importance in skeletal type of E-C coupling (Yamazawa 1997). The RYR2 gene, responsible for cardiac E-C coupling, is found on human chromosome 1 and expressed in cardiac muscle and brain tissue (Mikami 1989 and Otsu 1990). RYR3, unlike RYR1 and RYR2, appears to be widely expressed in smooth and skeletal muscle, brain, liver and testis. In muscle tissues RYR3 is probably activated by CICR, but does not appear to be critical for E-C coupling. In non-muscle tissue, RYR3 is co-expressed with IP_3 receptor, where it plays a role in intracellular Ca^{2+} homeostasis.

In smooth muscle and non-muscle tissues, the principal Ca^{2+} release function from intracellular Ca^{2+} stores is carried out by the IP_3 receptor, an analogue of the ryanodine receptor. The IP_3 receptor, although only about half of the size of the ryanodine receptor shares a high degree of molecular homology with the ryanodine receptor (Chadwick 1990).

In contrast to excitation, which is mediated by passive flux of Ca^{2+} ion into the cytosol via highly regulated Ca^{2+} release channels, relaxation requires the active transport of Ca^{2+} ions back into the SR. This process is accomplished by **SERCA Ca^{2+} pump**, which is densely packed in sarcotubular network of the SR (Arai 1994). The SERCA pump represents the major removal system of intracellular Ca^{2+} to levels sufficiently low (0.2-0.3 uM) to dissociate Ca^{2+} from troponin-C. The SERCA pump transports 2 Ca^{2+} ions for every ATP hydrolyzed.

The SERCA exists in several isoforms: SERCA1, SERCA2 and SERCA3 (Brandal 1986, Lytton 1988 and Burk 1989). SERCA2 is encoded by the ATP2B gene located on chromosome 12 (MacLennan 1987), which by alternative splicing produces two isoforms:

the shorter SERCA2a is expressed in cardiac and slow-twitch muscles and the longer form, SERCA2b, is expressed in smooth muscle and non-muscle tissues (Lytton 1988 and 1989). The cardiac form, SERCA2a encodes an integral protein of 115 kDa, predicted to form a protein of ten transmembrane segments (M1-M10) and two large cytoplasmic loops (between M3-M4 and M4-M5, respectively). The low resolution structure of the Ca^{2+} pump as determined by Toyoshima *et al.* (1993) reveals a complex structure composed of the head (ATP-binding and phosphorylation domains) and stalk domain attached to the transmembrane domain.

The most important regulator of SERCA activity is the level of cytosolic Ca^{2+}. The activity of SERCA2 pump is also regulated by phospholamban (PLB) in response to sympathetic stimulation. The regulatory activity of PLB is related to its phosphorylation state, where unphosphorylated PLB inhibits SERCA2, whereas PBL phosphorylation by PKA and CAM kinase reverses its inhibitory influence. PLB is expressed in cardiac, slow-twitch and smooth muscle tissues (Jorgensen 1987), as a single product of a gene located on human chromosome 6 (Fujii 1991). Phospholamban is a homo-pentamer, made up of subunits each having a molecular weight of 6.0 kDa. The C-terminal is hydrophobic and serves as a sarcoplasmic reticulum membrane anchor, whereas the N-terminal contains two phosphorylation sites (CaM kinase and PKA (Gasser 1988)), which when phosphorylated, stimulate Ca^{2+} transport.

1.6. Ca^{2+}-binding Proteins and Cardiac Function.

Transient increases in the intracellular levels of Ca^{2+} play a crucial role in regulation of contraction-relaxation cycling of a pumping heart. The Ca^{2+} coupled responses are coordinated by sets of Ca^{2+}-binding proteins involved in Ca^{2+} influx, efflux and storage. The aforementioned systems involved in intracellular Ca^{2+} increase, including: sarcolemmal and sarcoplasmic reticular Ca^{2+} channels, as well as, Ca^{2+} uptake systems: sarcolemmal NCX and sarcoplasmic reticular SERCA, are all Ca^{2+}-binding proteins. Moreover, the intracellular Ca^{2+} increases result in Ca^{2+} binding to troponin-C and calmodulin, the intracellular Ca^{2+} sensors, that regulate specific Ca^{2+} responses.

Ca^{2+} also binds to **sarcolemma** via non-specific electrostatic attraction to anionic and/or zwitterionic phospholipids (Philipson 1980). The manipulation of the net negative sarcolemmal charge with either polymyxin B (a highly positively-charged amphiphilic peptolipid) or phospholipase D (an enzyme catalyzing formation of negatively charged phosphatidic acids on phospholipids) results in displacement or augmentation of Ca^{2+} binding, respectively. The extent of Ca^{2+} binding to sarcolemma is an important determinant of contractile function, as Ca^{2+} binding to SL correlates with the force development (Bers 1979).

Binding of Ca^{2+} to proteins, on the other hand is mediated by high affinity association with an **'EF-hand'** motif or low affinity binding to **acidic side chain amino acids**. The 'EF-hand' motif consists of a 12 aa long evolutionarly conserved interhelical loop flanked by two perpendicularly oriented alpha-helices (helices E and F in parvalbumin (Kretsinger 1973) that together form a single Ca^{2+} binding site. The Ca^{2+}-binding is

coordinated by associations with the negatively charged oxygens from side chains of glutamates and aspartates, as well as uncharged oxygens of the main chain carbonyl groups. This motif is found in many proteins including troponin-C and calmodulin that function as cytosolic sensors of Ca^{2+} levels. Cardiac troponin-C, containing 3 'EF-hand' motifs, acts as a regulatory switch to cross-bridge cycling of actin and myosin. Calmodulin, on the other hand, has four 'EF-hand' motifs and exerts regulatory function on multiple effector targets. The molecular mechanism of the 'EF-hand' switch involves a configurational change upon complexing with Ca^{2+}, that increases surface hydrophobicity required for efficient interaction with a specific effector target.

An 'EF-hand' motif is also found in the L-type Ca^{2+} channels encoded by genes of class C, D and S (Tsien 1991 and Krogh 1994). Interestingly the location of 'EF-hand' motif coincides with the region of DHP binding site, that is highly conserved and evolutionarly preserved in L-type Ca^{2+} channels. It is believed that Ca^{2+} binding to the 'EF-hand' induces a conformational change allowing binding of dihydropyridine (Tsien 1991).

Cardiac dyadic junctions of T-tubules and SR contain a 22-kDa Ca^{2+}-binding protein, called sorcin, that contains four 'EF-hand' motifs (Wang 1995). Sorcin associates with Ca^{2+} release channel/RyR receptors (Meyers 1995) and modulates Ca^{2+} release channel function (Lokuta 1997). The elucidation of the exact role of 'EF-hand' motifs on the regulation of RyR receptors remains to be determined.

The **'non-EF-hand'** Ca^{2+} binding proteins include lumenal Ca^{2+} storage proteins of SR as well as integral Ca^{2+} buffering proteins of SL and SR. **Calsequestrin** (CS) is a

major intralumenal protein of SR, that binds large amounts of Ca^{2+} with low affinity. CS is highly enriched in the subsarcolemmal cisternae, where it is co-localized with the Ca^{2+} release channel via interaction with triadin (McLeod 1991). By binding to both, the Ca^{2+} release channel and CS, triadin organizes the Ca^{2+} release complex (Guo 1996). The Ca^{2+} release complex also includes junctin (a CS-binding protein), however its function remains unclear (Jones 1995). There are two isoforms of CS encoded by two different genes. Cardiac CS is a product of CAQ2 gene expressed in cardiac and slow-twitch muscles (Scott 1988), whereas skeletal type encoded by CAQ1 gene is found in fast- and slow-twitch muscle (Fliegel 1987 and 1989a). Both CS isoforms are highly acidic (29% of residues are acidic) and undergo conformational change upon binding to Ca^{2+}.

In addition to CS, several other Ca^{2+}-storage proteins exist in SR. **Sarcalumenin** (Leberer 1989a), also a highly acidic glycoprotein (25% of residues are acidic), is localized in the non-junctional SR (Leberer 1990). Sarcalumenin is encoded by a single gene which by alternative splicing yields two glycoproteins of 160 and 53 kDa. A truncated 53 kDa product lacks the N-terminal containing acidic residues, however, similar to the 160 kDa product, it is also distributed in the non-junctional SR (Leberer 1989a, 1989b and 1990). Another protein Ca^{2+}-binding protein called **histidine-rich Ca^{2+} binding protein** was identified in the lumen of the SR. Negatively charged amino acids which account for 44% of all residues are believed to participate in Ca^{2+} binding (Hofmann 1989a and 1989b).

In non-muscle tissues, where calsequestrin is not expressed, the luminal Ca^{2+} binding may instead be carried by **calreticulin** (Smith 1988 and Fliegel 1989b). The

highly acidic C-terminus, similar to that found in calsequestrin, may account for high capacity Ca^{2+} binding of calreticulin.

By far the most abundant Ca^{2+}-binding protein of intralumenal SR is CS. However, the internal loops of **integral membrane proteins** bearing acidic amino acid residues may also attribute to Ca^{2+} binding. For example 4-10 acidic amino acids stretches in the ryanodine receptor and the Ca^{2+} pump (MacLennan 1985, Takeshima 1989 and Zorzato 1990). Given the abundance of Ca^{2+} ATPase in SR (approximately 50% of total SR protein) the putative Ca^{2+}-binding sites may play a role in the Ca^{2+} transport.

It is possible, that a specific type of Ca^{2+}-binding protein, its relative amount and specific localization may be relevant not only to the Ca^{2+} buffering, but also in regulation of Ca^{2+} homeostasis. Studies of Ca^{2+} loading of SR revealed that the presence of Ca^{2+}-precipitating anions (oxalate or phosphate) in SR increase Ca^{2+} uptake by SERCA (Feher 1980) and conversely high Ca^{2+} concentrations markedly inhibit SERCA activity. The structural compartmentalization of SR and its intralumenal Ca^{2+}-binding proteins may, therefore, define concentration gradients critical for functional optimalization of mechanisms involved in SR Ca^{2+} fluxes which determine transient increases in cytoplasmic Ca^{2+} concentration during the relaxation-contraction cycling.

1.7. Statement of the Problem.

In view of the importance of Ca^{2+} binding proteins in the E-C coupling, the Ca^{2+} binding properties of highly purified cardiac sarcolemmal membranes were investigated. Two Ca^{2+}- binding glycoproteins of 97 and 125 kDa, that co-purified with DHP receptor/L-type Ca^{2+} channel, were identified. Further efforts directed toward molecular characterization of these glycoproteins lead to isolation of novel cDNAs from rabbit cardiac expression libraries. This approach resulted in characterization of a novel family of proteins (Demchyshyn 1990 and Wigle 1997) referred to as SLAPs encoding sacrolemmal associated protein (SLAP). The deduced protein structure of SLAPs predicted an extended coiled-coil with two leucine zippers and a carboxyl terminal transmembrane domain. The SLAP was defined as an acidic alpha-helical coiled-coil membrane protein. There was no putative 'EF-hand', however, there was a negative glutamate stretch at the C-terminal which may possibly bind positive ions, such as Ca^{2+}.

SLAPs are encoded by a single gene mapped to a human chromosome 3p14.3-21.2 (Wigle 1997). Northern blot analysis demonstrated expression of three SLAP transcripts of 5.9, 4.6 and 3.5 kb in cardiac muscle. Subsequent studies identified three SLAP cDNAs (SLAP1, SLAP2 and SLAP3) thought to correspond to the three observed transcripts. Northern blot analysis and sequencing of the cDNA clones revealed that SLAP transcript diversity arises due to alternative usage of the N-terminal sequences thus generating three SLAP isoforms. The topology of SLAP isoforms is depicted in Figure 1. The open-reading frame of the largest SLAP isoform, SLAP3, is 2316 nt long. SLAP3 is predicted to encode a 772 aa protein. In SLAP1 and SLAP2 the N-terminal is

Figure 1. Topology of SLAP Isoforms.

SLAPs are a family of sarcolemmal-associated proteins encoded by a single gene. Previous studies have identified three SLAP isoforms: SLAP1, SLAP2 and SLAP3 containing a common C-terminus and the N-terminals of variable lengths. All SLAPs are predicted to form extended coiled-coil structures with two leucine zipper motifs and a C-terminal transmembrane domain.

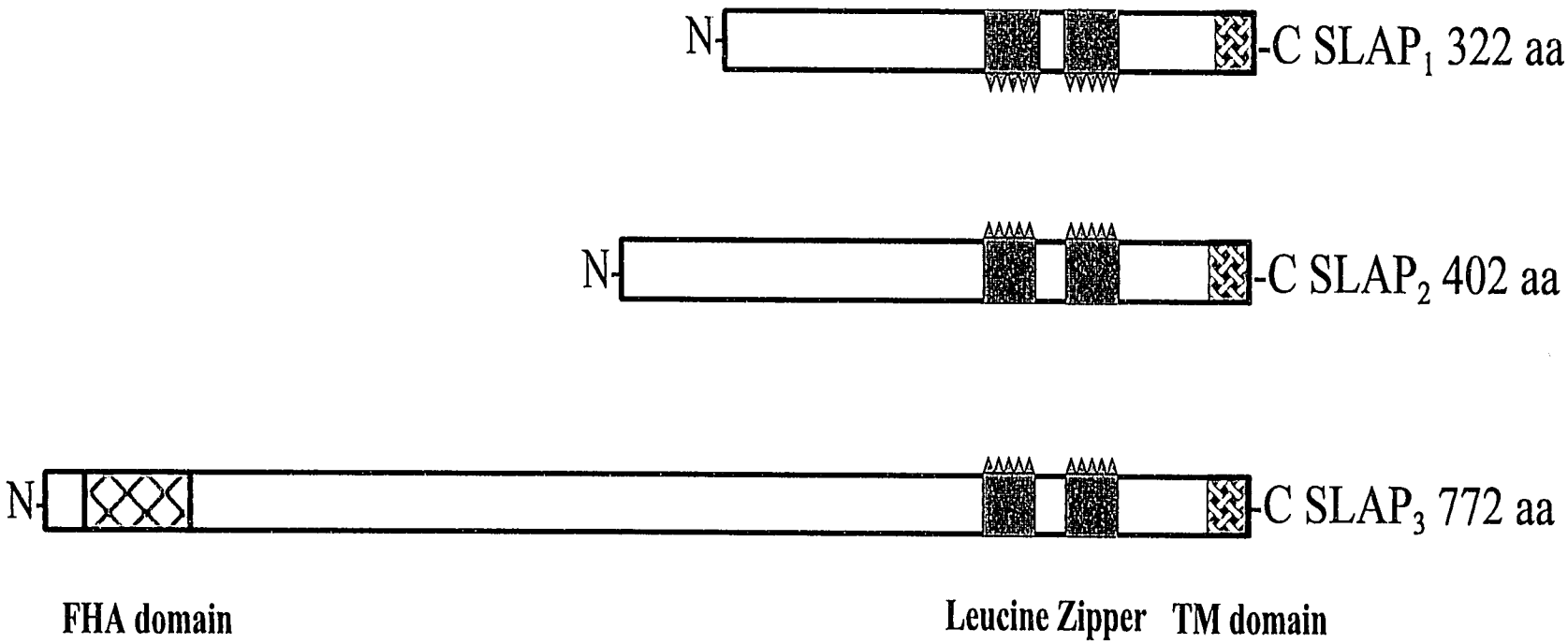

FHA domain - a nuclear signalling domain
Leucine Zipper - a protein-protein interaction domain
TM domain - a transmembrane domain

shorter, giving rise to 322 and 402 aa long polypeptides. All of the SLAP isoforms are predicted to form coiled-coil structures, contain two leucine zipper motifs and all terminate at a common stop codon.

Specific antisera raised against SLAP, recognized four polypeptides in cardiac membrane fractions. The immuno-histological localization studies demonstrated that SLAPs localize not only to the cell membrane, but also to the T-tubules and SR. In light of observed sequence diversities in SLAP cDNAs the molecular mechanisms that give rise to the multiple SLAP isoforms needed to be investigated. Studies in the thesis were carried out to determine the genomic organization of the 3' end of the SLAP gene and to investigate the alternative splicing of the SLAP primary transcript in the areas of sequence divergency.

Materials and Methods

2.1. Nucleic Acid Preparations.

(i) Isolation of total RNA by TriPure Method.

Total RNA was extracted from rabbit and rat tissues using the TriPure isolation reagents (Boehringer Mannheim, Laval, PQ, Canada) according to methodology described by Chomczynski (1993). Tissues were harvested and immediately frozen in liquid nitrogen and later stored at -80°C until further processing. The tissues were pulverized in liquid nitrogen using a mortar and pestle. The powdered tissues were added to a solution of TriPure (1 ml per 100 mg of tissue) and subjected to homogenization with a power polytron at a high speed (3 min at a setting 8). The homogenate was centrifuged at 4°C (10 min at 12,000 rpm) to remove the extracelluar membrane, polysaccharides and high molecular weight DNA. The supernatant (containing RNA) was transferred to a fresh polypropylene tube and incubated at room temperature to allow the complete dissociation of nucleoprotein complexes. Subsequently, chloroform was added (0.2 ml per 1.0 ml of TriPure used) and the mixture was vortexed and then incubated for 10 min at room temperature. The homogenate was then centrifuged to separate the organic phases. The upper aqueous phase was collected and isopropanol was added (0.5 ml per 1.0 ml of TriPure) to precipitate RNA. Following incubation at room temperature for 10 min, the sample was centrifuged at 4°C (10 min at 12,000 rpm). The RNA pellet was washed with 75% EtOH (1.0 ml per 1.0 ml of TriPure) and centrifuged at 4°C (5 min at 7,500 rpm).

The pellet was air dried and resuspended in DEPC-treated ddH_2O. Concentration and purity of RNA were assessed by a photospectrometer reading (Beckman, Palo Alto, CA, USA) at 260 nm and 260nm/280nm ratio, respectively. All RNA samples were stored at -80°C until use.

(ii) Isolation of DNA.

(a) Alkaline Lysis Plasmid Miniprep.

Quick-and-Dirty miniprep method is used for an isolation of plasmid DNA ($OD_{260}/OD_{280} < 1.5$) suitable for the restriction enzyme digestion to determine insert size and orientation. The protocol is a modification of Sambrook *et al.* (1989). Transformed DH5-α cells were inoculated into 7 ml of LB broth (Difco, Detroit, MI, USA) containing 75 μg/ml of ampicillin (Life Technologies, Mississauga, ON, Canada) and incubated overnight at 37°C with vigorous shaking at 225 rpm. 2 ml of the overnight culture was centrifuged and the bacterial pellet was resuspended in 200 μl of solution 1 (RNase-A, glucose, Tris-HCl and EDTA). The bacteria were incubated on ice for 5 min, and then 400 μl of solution 2 (1.0% SDS, 0.2N NaOH) was added to lyse and the sample was gently mixed by inversion. The cells were then incubated on ice for 5 min prior to addition of 300 μl of solution 3 (7.5 M Ammonium Acetate). Samples were then incubated on ice for 5 min followed by a centrifugation at 14,000 rpm to pellet cellular debris and chromosomal DNA. The supernatant was transferred to a new microcentrifuge tube and 1 ml of isopropanol was added. Following vortexing samples were allowed to stand at room temperature for 5 min and then were centrifuged at 14,000 rpm for 10 min.

The supernatant was discarded and the plasmid DNA pellets were washed twice with ice cold 70% ethanol. DNA was air dried and resuspended in 50 μl of TE. The samples were stored at -20°C until use. 3 μl of the isolated plasmid was used for restriction enzyme digestion.

(b) QIAGEN Plasmid Miniprep.

The Qiagen plasmid miniprep (QIAGEN, Mississauga , ON. Canada) was used to isolate a high purity DNA (>1.7 OD_{260}/OD_{280}) suitable for a variety of applications including: cycle-sequencing, cDNA probe synthesis, ligation, transformation and restriction enzyme digestion. QIAprep Plasmid Kit procedure is based on the modified alkaline lysis method by Birnboim and Doly (Birnboim 1979), and on the absorption of DNA onto silica in the presence of high salt (Vogelstein 1979).

Similarly to Quick-and-Dirty protocol, transfected DH5-α were inoculated in LB broth with ampicillin (75 μg/ml) and grown overnight (12-16 hrs) at 37°C with vigorous shaking at 225 rpm. The cells were harvested by centrifugation at 14,000 rpm for 5 min. The bacterial pellet was resuspended in 250 μl of P1 buffer by vortexing. 250 μl of buffer P2 was then added and mixed gently by inversion. When the solution became viscous and slightly clear, buffer N3 was added and samples were gently mixed by inversion. Samples were then centrifuged to pellet the chromosomal DNA and cellular debris at 14,000 rpm for 10 min. The supernatant was transferred to a QIAprep spin column and centrifuged for 30 sec at 14,000 rpm. The flow-through was discarded and 500 μl of buffer PB was applied to each spin column and spined for 30 sec. Subsequently, 750 μl of PE buffer was

applied to each of the QIAprep spin columns followed by centrifugation for 30 sec. To remove the residual PE buffer, the columns were re-centrifuged for 1 min. The QIAprep columns were then placed in clean 1.5 ml microcentrifuge tubes and 50 μl of 10 mM Tris-HCl (pH 8.5) was used to elute plasmid DNA. All samples were stored at -20°C, until use. For restriction enzyme digestion 2 μl of the plasmid DNA was used. For other applications plasmid DNA was first quantified and then used in accordance with the specific protocols.

(c) Small-Scale Phage DNA Isolation.

This procedure is a modification of small-scale liquid lysate protocol from Current Protocols in Molecular Biology (Ausubel 1995). The protocol is useful for purification of small quantities of bacteriophage DNA for restriction enzyme analysis and subcloning. The phage are concentrated by centrifugation and capsids were destroyed with phenol. The phage DNA is then ethanol precipitated.

A single phage plague was cored out and eluted in 400 μl of SM buffer and 10 μl of chloroform for 2 hrs at 4°C. 10 μl of the eluted phage was then used to infect 100 μl of host bacterium at 37°C for 15 min. The phage and bacteria were subsequently mixed with NZCYM top agarose and plated out on large bacterial plates containing NZCYM agar (Difco). The plate were incubated overnight at 37°C. Once the plaques reached confluence, the top agarose layer was scraped off and transferred to a 50 ml conical tube containing SM buffer. The mixture was vortexed and phage was allowed to elute for 2 hrs at 4°C. Subsequently the mixture was centrifuged at 3,000 rpm at 4°C to pellet the agarose

and the supernatant containing phage was transferred to a clean 50 ml conical tube. Subsequently, 0.05 mg of DNase and 0.25 mg of DNase-free RNaseA were added to the liquid phage lysate and incubated at 37°C for 1 hr to degrade bacterial nucleic acid. The sample was then centrifuged for 90 min at 27,000 rpm at 4°C in a SW-28 rotor (Beckman). The supernatant was discarded and tubes inverted on paper towels to remove remaining liquid. The small translucent phage pellet was resuspended in 400 μl of TE by vortexing. Subsequently, 400 μl of buffered phenol was added to open phage capsids and the mixture was gently vortexed for 20 min and then centrifuged at 14,000 rpm for 2 min. The aqueous layer was re-extracted with phenol and transferred to a clean tube. The aqueous layer was then twice extracted with 400 ul of chloroform. Subsequently, 40 μl of 3 M NaOAc (pH 4.8) and 800 μl of ice cold 100% EtOH were added to precipitate phage DNA. The mixture was incubated at room temperature and centrifuged at 14,000 rpm for 5 min to pellet the phage DNA. The DNA pellet was twice washed with 70% ice cold EtOH and air dried. The pellet was resuspended in 200 μl of TE (pH 8.0) and stored until use. For restriction enzyme digestion 10-15 μg of phage DNA was used.

2.2 RT-PCR.

The RT-PCR is a two-step procedure used for generation of DNA products from RNA templates. In the RT (reverse transcriptase) reaction the first strand cDNA is synthesized, in PCR (polymerase chain reaction) stage on the other hand, DNA is exponentially amplified.

(i) First-Strand cDNA Synthesis (RT).

1 μg of total RNA isolated by TriPure method and 0.10 μg of random hexamers (Life Technologies) were incubated at 70°C for 10 min and snap cooled on ice. Subsequently, following components were added to the mixture to obtain a final concentration of 50 mM Tris-HCl, 75 mM KCl, 3 mM $MgCl_2$, 0.01 DTT and 500 μM of each of the dNTPs (dATP, dCTP, dGTP, dCTP and dTTP (Pharmacia, Uppsala, Sweden)) in a 20 μl reaction. The reaction mixture was temperature equilibrated at 37°C for 2 min, prior to addition of 200 U of SuperScript™ RNase H$^-$ Reverse Transcriptase (Life Technologies). The RT reaction was carried out at 37°C for 60 min, followed by enzyme inactivation at 95°C for 10 min.

(ii) Polymerase Chain Reaction (PCR).

PCR analysis was performed with corresponding sets of primers summarized in Table 1. Oligonucleotides were chosen to span regions of SLAP sequence divergence. The primer design utilized OligoTech software tool to calculate melting temperature of primers and to assess homo- and heterologous associations (stem-loop structures). The primers were synthesized at the University of Ottawa Biotechnology Institute (Ottawa, ON, Canada). The PCR reaction consisted of 10 μl of first-strand cDNA reaction mixture, 20 mM Tris-HCl (pH 8.4), 50 mM KCl, 1.5 mM $MgCl_2$, 400 nM of each primer and 1 Unit of Taq DNA Polymerase (Pharmacia) in a total volume of 50 μl. All of the PCR amplifications included a manual 'hot start' to minimize non-specific priming. The 'hot start' involved heating of the reaction mixture to 80°C prior to addition of Taq polymerase.

TABLE 1. Primers Utilized in RT-PCR Analysis of SLAP.

Table of primers used for RT-PCR analysis of SLAP sequence diversities in the SLAP2/3 region as well as in the 5' and 3' regions of SLAP1, common to all SLAPs. The position of the primers is given relative to the longest SLAP cDNA clone, SLAP3. The 'S' denotes the sense orientation, whereas 'AS' an antisense.

Region	Name	Primer Sequence (5'->3')	Position[a]	Orientation[b]
SLAP2/3	SLAP3.F	AATGAAAGGCTAACAGC	1472-1488	S
	SLAP3.R	CCTCCACGATCAGC	1563-1577	AS
SLAP1 5'	5'.F	GGGAATTCATGGATGAGCAAGACCTG	1709-1726	S
	5'.R	TCTCGAGGCTGCTTGATGAAGGAGC	1942-1956	AS
SLAP1 3'	TM.F	TCTCGAGTCAATCACAGATGAGCTC	2516-2533	S
	TM.R	TGAATTCCCTCTTTACAGACAGATAC	2834-2852	AS

[a]Position given relative to SLAP3 cDNA sequence
[b]Strand orientation: sense (S), antisense (AS).

The MJ Research thermocycler (Watertown, MA, USA) was used and PCR cycling conditions were optimized for each primer pair and the size of amplified product.

(a) Amplification of 5' Variants.

To amplify 5' alternative region of SLAP, 5'.F and 5'.R primers were used (see Table 2). The PCR conditions included the first denaturation at 94°C for 3 min followed by cycling conditions of 94 °C for 45 sec, 52 °C for 45 sec and 72 °C for 1 min, and a final elongation at 72 °C for 10 min. The PCR reaction consisted of 30 cycles.

(b) Amplification of TM Variants.

TM variants were amplified with TM.F and TM.R primers (Table 2). The cycling conditions consisted of a denaturation at 94°C for 45 sec, annealing at 52 °C for 45 sec and an elongation at 72 °C for 45 sec. 30 cycles were performed.

(c) Amplification of SLAP3 Variants.

To amplify SLAP3 variant region **S3.F and S3.R** primers were used (see Table 2). The cycling conditions consisted of: 94 °C for 30 sec, 50 °C for 30 sec and 72 °C for 25 sec, repeated 30 times.

2.3. Agarose Gel Electrophoresis.

25 μl of the PCR reaction or 20 μl of the restriction enzyme digestion was electrophoresed through TAE-agarose gel (BioRad, Hercules, CA, USA) at 100V in an

Owl Scientific electrophoresis apparatus (Woburn, MA, USA). Ethydium bromide (Boehringer Mannheim) staining was used for visualization of the DNA. The size of the products was estimated by size comparison to 100 bp, 1.0 kb and λ-HindIII ladders (Life Technologies).

2.4. Subcloning of PCR Generated 5' and TM Variants.

PCR products were extracted with chloroform and then ethanol precipitated (0.1 volume NaOAc pH 4.8 and 2.5 volumes of ice cold 100% EtOH) to remove Taq Polymerase and remaining primers. DNA pellets were resuspended in sterile dH_2O and subjected to double restriction digestion with *EcoR1* and *Xho1* (Pharmacia) at 37°C for 1 hr. The digests were electrophoresed through 1.5% low-melt agarose gel at 80 V for 2 hr. The PCR products were gel purified and snap-frozen in liquid nitrogen. The gel slices were centrifuged at 14,000 rpm at 4°C for 15 min. 5 μl of the gel slice supernatant, containing eluted PCR products, was then subcloned pBlueScript KS vector (Stratagene, La Jolla, CA, USA) predigested with *EcoR1* and *Xho1*.

2.5. DNA Ligation.

PCR fragments and restriction enzyme digestion fragments were electrophoresed through regular 1% agarose (BioRad) TAE mini-gels and gel purified. The gel slices were then treated with the GeneClean (Bio/Can Scientific, Mississauga, ON, Canada) glass milk purification procedure.

For the ligation of 'sticky ends' products, the purified fragments were ligated into

either of pUC18/19 (Pharmacia), pTZ18/19 (USB, Cleveland, OH, USA) or pBlueScript KS (Stratagene) vectors predigested with appropriate restriction enzymes and dephosphorylated with Calf Intestine Phosphatase (Life Technologies). The 'sticky end' ligation were performed at 15°C for 1 hr with 1 U of T4 ligase (Life Technologies) in a total volume of 20 μl. The 'blunt-end' ligations, on the other hand were performed overnight.

2.6. Preparation of DH5-alpha Competent Cells.

Bacterial stock, stored at -80°C, was stricked with a loop on an LB plate (without antibiotic) and incubated overnight (12-16 hr) at 37°C. Next day, a single colony was selected and used to inoculate 5 ml of LB broth. On the third day, the overnight culture was transferred to 100 ml of LB broth and grown for 2-3 hr. When the bacterial culture reached an optical density of 0.5 at OD_{600}, the culture was chilled on ice for 15 min and then centrifuged at 4,000 rpm for 10 min at 4°C. The supernatant was decanted and the bacterial pellet was gently resuspended in 20 ml of solution B (30 mM KoAc, 100 mM RbCl (99%), 10 mM $CaCl_2.H_2O$, 50 mM $MuCl_2.4H_2O$, 15% glycerol, pH 5.8, sterilized by filtration). Resuspended cells were left on ice for 15 min and then centrifuged again at 4,000 rpm for 10 min at 4°C. The supernatant was removed and the bacterial pellet was resuspended in a solution C (10 mM MOPS, 75 mM $CaCl_2$, 15% glycerol, pH 6.5 sterilized by filtration) by gentle vortexing. The bacterial suspension was immediately aliquoted into pre-chilled, sterilized eppindorf microcentrifuge tubes and stored at -80°C until use.

2.7. Transformation.

20 μl of ligation reaction was added to DH5-α competent cells and allowed to incubate on ice for 30 min. Subsequently, the cells were heat shocked at 42°C for 30 sec to take up the plasmid. Following a 2 min incubation on ice, 150 μl of LB broth (without ampicillin) was added to each sample. A 1 hr incubation at 37°C with shaking at 225 rpm followed. Each sample was then plated on LB agar plates containing ampicillin (75 μg/ml) and X-gal (Life Technologies) for α-complementation. The bacterial plates were incubated overnight (12-16 hr) at 37°C and next morning white recombinant colonies were selected for further manipulation.

2.8. Miniprep Screening of Clones.

White recombinant bacterial colonies were grown overnight in LB broth (with 75 μg/ml of ampicillin) and plasmid DNA was isolated by Quick-and-Dirty method. 5 μl of plasmid DNA was digested with the appropriate restriction enzymes (Pharmacia and Life Technologies). The digests were electrophoresed through an agarose gel to verify the presence or orientation of the inserts. The positive clones were selected for further manipulation.

2.9. Cycle Sequencing.

ABI Prism™ Dye Terminator cycle sequencing (Perkin-Elmer, Mississauga, ON, Canada) was used for a rapid and highly efficient enzymatic DNA sequencing reaction. Plasmid DNA clones were purified by QIAgen miniprep method and DNA was quantified by a photospectrometer reading at 260 nm. The reaction mix contained: 500 ng of template DNA, 3.2 pmol of primer and 8 ul of the terminator ready mix containing dye-labeled terminators and AmpliTaq DNA Polymerase (FS). The sequencing reaction was performed 25 times under following cycling conditions: 96°C for 30 sec, 50°C for 15 sec and 60°C for 4 min. Following cycle-sequencing samples were EtOH precipitated to remove residual dyes and the sequencing products were resuspended in a formamide prior to loading on polyacrylamide sequencing gel. The sequence analysis was carried out by University of Ottawa Biotechnology Institute using ABI DNA sequencer and ABI Prism 310 Genetic analyzer (Perkin-Elmer).

The sequencing results were then analyzed with SeqaidII (University of Kansas), PROSITE (Appel 1994), PSORT (Nakai 1992) and BLAST (Altschul 1990).

2.10. Screening of Libraries.

(i) Titration of a Library.

In order to determine a titer of a library, 1 μl of the library was sequentially diluted in SM buffer. Dilutions of 10^{-4} to 10^{-9} were plated on NZCYM plates and incubated overnight (10-14 hr) at 37°C. Next day, plaques were counted and the titer of the library was determined.

(ii) Plating and Lifts.

Bacterial host culture following an overnight inoculation in NZCYM broth with 0.2% maltose was centrifuged and resuspended in 10 mM $MgSO_4$. 200 μl of host was infected with 50,000-60,000 pfu of phage (in 100 μl of SM) and incubated at 37°C for 15 min. Subsequently cultures were mixed with 7 ml of NZCYM agarose and plated on NZCYM plates. The library plates were then inoculated for 8-10 hrs, until the plaques almost reached confluence. Plates were, then transferred to a 4°C cold room for 30 min, prior to the library lifting onto nylon membranes (NEN, Boston, MA, USA). Each plate was lifted in duplicate. The membranes were, then subjected to a denaturating solution (0.5M NaOH, 1.5M NaCl) for 5 min, followed by a neutralization solution (1.0M Tris-HCl pH 8.0, 1.5M NaCl) for 5 min and a final wash (2X SSC) for 5 min. The membranes were air dried and DNA was covalently cross-linked to the membranes by UV irradiation.

(iii) Hybridization.

The filters were individually wetted and prehybridized in PEG hybridization solution (10% PEG, 7% SDS, 1.5X SSPE) at 65oC for 2 hr in a hybridization oven (InterScience, Markham, ON, Canada). Subsequently, fresh PEG hybridization solution containing a cDNA probe was added (1-5x10^6 cpm/ml) and allowed to incubate at 65°C for 16 hrs.

(iv) cDNA Probe Synthesis.

Complementary DNA fragments used as templates for probe synthesis were generated by restriction enzyme digestion or PCR amplification. cDNA templates were electrophoresed through 1% low-melt agarose gels and gel purified by the snap-freeze method or with GeneClean glass milk. 25 ng of template DNA was used for random primer labeling with 50 μCi of [alpha-^{32}P]dCTP (NEN) using a Ready-Prime kit (Amersham, Arlington Hts, IL, USA). The template DNA was heat denatured at 94°C for 5 min and added to the Ready-Prime tube, containing dNTPs and enzyme. The radioactive label was then added and the mix was incubated at 37°C for a minimum of 10 min. Prior to addition of the probe to the hybridization buffer, the probe was first heat denatured by boiling for 10 min and then snap cooled on ice.

(v) Washing Conditions and Autoradiography.

Following overnight hybridization, the membranes were washed at room temperature with a low stringency wash (0.1% SDS, 1.0X SSC) to remove the unincorporated probe. Then, in the next washes salt concentration and temperature were varied to increase the ratio of specific probe binding to non-specific background. The membranes were then exposed to KODAK BioMax MR films (Eastman Kodak Company, Rochester, NY, CA) with intensifying screens at -80°C for 8-16 hr. The films were developed with automated KODAK X-OMAT machine at Ottawa General Hospital (Ottawa, ON, CA).

(a) Screening of Rabbit Genomic Library.

Rabbit lambda DASH^{R}II genomic library (Stratagene) was tittered and 1.4X10^6 pfu were plated on 24 NZCYM plates. Each plate contained 60,000 pfu. The plates were lifted in duplicate. Following cross-linking, the membranes were pre-hybridized and hybridized in PEG hybridization buffer at 55°C. A restriction enzyme digestion fragment of SLAP was ^{32}P-radiolabelled by random primer labeling method. The hybridization was carried out overnight at 55°C. Next day filters were washed twice at 37°C for 10 min in low stringency wash (0.1% SDS, 1.0X SSC), twice at 50°C for 15 min in a high stringency wash solution (0.1% SDS, 0.1X SSC) and exposed overnight to Kodak BioMax MR films. The positive clones were isolated by re-screening of the primary positive clones and finally phage DNA was obtained by the small-scale phage isolation method.

b) Screening of Mouse Genomic Library.

A lambda DASH^{R}II mouse genomic library (mouse strain 129) generously donated by Dr. J. Bell was tittered and 0.5x10^6 pfu were plated out on NZCYM plates. The library was lifted in duplicate and the membranes were pre-hybridized and hybridized at 42°C in 50% formamide, 6X SSPE, 0.5% SDS, 5X Denhardt and 0.1 mg/ml of herring sperm DNA. A *SalI-EcoRI* restriction enzyme fragment of SLAP3 (1-3017) was used as a probe. Following overnight incubation membranes were washed twice at room temperature with 5X SSC and 0.1% SDS for 5 min, and twice at 50°C with 2X SSC and 0.1% SDS for 15 min. The membranes were then exposed to Kodak BioMax MR films for 16-24 hrs. The positive clones were isolated and analyzed by Southern Blotting.

c) Screening of Human Cardiac cDNA Library.

Human heart lambda ZAPII cDNA library (Stratagene) was titrated and $1.0X10^6$ pfu were plated on 20 NZCYM plates. The library was lifted in duplicate and DNA was cross-linked to the NEN nylon membranes. The membranes were pre-hybridized in PEG solution at 65°C for 2 hrs. The *Sal1- EcoR1* restriction fragment of SLAP3 (1- 3017 nt) was used as a probe. The hybridization was performed in PEG hybridization solution at 65°C overnight. Next day the membranes were washed twice at room temperature for 10 min (0.1% SDS, 1.0X SSC) and twice at 60°C for 10 min in 0.1% SDS and 0.1X SSC. The autoradiography was performed using Kodak BioMax MR film with intensifying screens at -80°C for 16-24 hrs.

2.11. Southern Blot Analysis.

Souther blot analysis was performed to identify SLAP exons in the restriction enzyme digest fragments of the phage genomic DNA clones. Phage DNA clones were digested with specific enzymes and electrophoresed through 1% agarose gel. The DNA was denatured by soaking the gel in 1.5 M NaCl and 0.5 M NaOH for 1 hr at room temperature. The gel was then neutralized by soaking the gel in a solution of 1 M Tris-HCl (pH 8.0) and 1.5 NaCl for 1 hour. The gel was then blotted onto MSI nylon membrane (MSI, Westboro, MA, USA). The following day, the membrane was air dried and DNA was covalently cross-linked to nylon by irradiation with UV. The membrane was prehybridized in PEG solution for 2 hour at 65°C. The prehybridization buffer was removed and replaced with a hybridization PEG buffer containing a ^{32}P-radiolabelled

probe. The hybridization was performed overnight at 65°C. Next day the blot was washed as follows:

(a) low stringency (0.1%SDS, 1.0X SSC) for 5 min at room temperature.

(b) low stringency for 15 min at 50°C.

(c) high stringency (0.1% SDS, 0.1X SSC) for 15 min at 60°C.

The membrane was then sealed in a plastic bag and exposed to Kodak BioMax MR films with intensifying screens at -80°C.

RESULTS

3.1. Genomic Organization of SLAP.

In order to determine the genomic organization of the 3' end of SLAP gene, common to all SLAP isoforms, a rabbit lambda DASHII genomic library was screened with a ^{32}P-radiolabelled 319 nt HindIII-AvaI restriction enzyme fragment of SLAP3 (1607-1926). Screening of $1.3X10^6$ pfu yielded three non-overlapping clones R-2g, R-13g and R-14g. The genomic clones were digested with restriction enzymes and analyzed by Southern blot hybridization to identify restriction fragments containing SLAP exons. The positive fragments were subcloned and subjected to further analysis by restriction enzyme digestion to generate smaller fragments of suitable length for sequencing. As an example of this approach the isolation of exon V is summarized in Figure 2. Employment of this approach allowed to isolate SLAP exons in the 3' end of the gene and to determine their length and exon-exon boundaries.

Analysis of the genomic DNA clones led to isolation of exon I in clone R-14, exons II and III in R-2 and exons V to IX in R-13. The relative length of the SLAP exons and the relative position of the exon-exon boundaries in the SLAP cDNA sequence is shown in Figure 3. Sequencing of the identified exons which allowed the elucidation of the exon-intron junctions is summarized in Table 2. The 3' end of SLAP gene extending from nucleotide 1560 to 2575 is composed of at least 8 exons ranging in size from 60 nt to 321 nt. The introns, on the other hand, range in size from 0.2 kb to more than 5.5 kb. All of the introns identified start with a 'gt' and end with an 'ag' thus complying with the intron GT-AG rule (Mount 1982).

Figure 2. Isolation of exon V.

Restriction enzyme digestion of the R-13 genomic clone with *EcoR1* and *Xba1* followed by Southern blot analysis with a SLAP probe (*HindIII-Pst1*: 1607-1845) suggested the presence of exon V in the 4.5 kb *Xba1* restriction fragment (see panel A). Following subcloning of the fragment into pBlueScript KS vector further restriction enzyme analysis was performed with *EcoR1, Sst1, Kpn1, BamH1, Pst1 and HindIII* enzymes (pannel B). Exon V was confined to a 2.0 kb *BamH1* subfragment depicted by *cross-hatched area.* Following subcloning of the subfragment into pUC19 vector the construct was sequenced. Panel C depicts a cycle-sequencing tracing where *underlined* sequence represents the exon V sequence. The exon V is 75 nt long and the 5' and 3' flanking introns contain the consensus dinucleotides 'ag' and 'gt', respectively.

A)

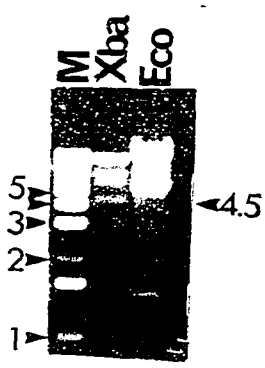
M
Xba
Eco
5
3
2
1
4.5

B)

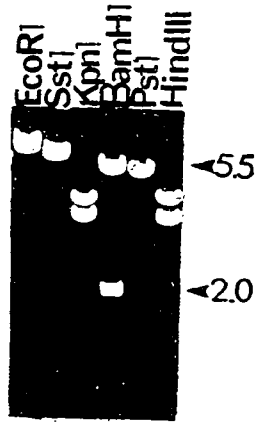
EcoRI
SstI
KpnI
BamHI
PstI
HindIII
5.5
2.0

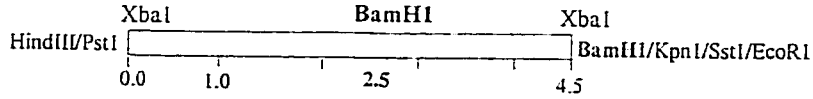
XbaI
BamHI
XbaI
HindIII/PstI
BamHI/KpnI/SstI/EcoRI
0.0
1.0
2.5
4.5

C)

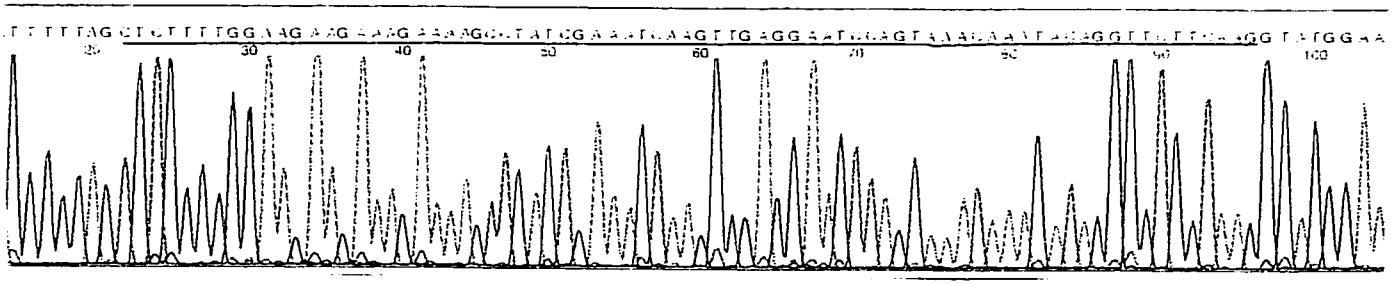

Figure 3. Length and Relative Positions of SLAP Exons.

Isolation and sequencing of the SLAP exons allowed to determine the length of the individual exons as well as to establish the exon-exon boundaries of the 3' end of the SLAP gene (1560-2675). SLAP exons are denoted in *roman numerals*, whereas the numbers *in italics* located above the exons indicate the length of the respective exons (in bp).

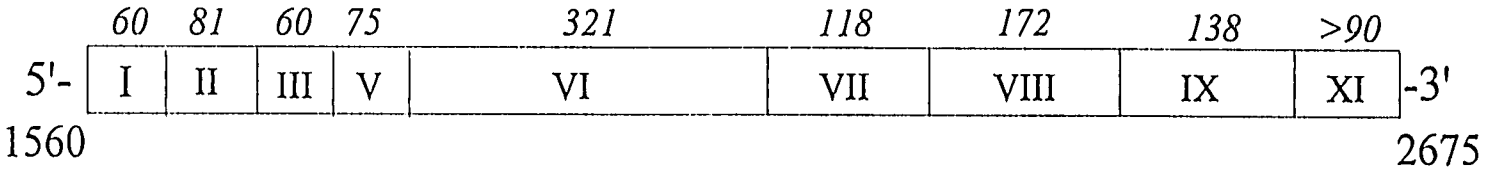
60
81
60
75
321
118
172
138
>90
5'-
I
II
III
V
VI
VII
VIII
IX
XI
-3'
1560
2675

TABLE 2. Compendium of Intron-exon junctions of the 3' end of the SLAP gene.

Direct sequencing of the SLAP exons as well as of the respective ends of the 5' and 3' flanking introns allowed elucidation of the intron-exon junctions of the 3' end of the SLAP gene. Exons are denoted in *uppercase* and numbered in *roman numerals*, whereas introns are denoted in the *lowercase* and numbered in *arabic numerals*. All of the introns contain dinucleotide consensus sequences 'gt' and 'ag' at the 5' and 3' ends of the introns, respectively.

No.	Size bp		No.	Size kb		
-	--	.....	1	>3.5	tctttggcagAGAAGCTGA	I
I	60	TTGCAAAAGgtcgttttct	2	>2.0	ctctctgtagAAAACCAGG	II
II	81	ACACTACGGgtgagtttta	3	0.2	cctctcgaagACGCCCAAA	III
III	60	TATTAAAAGgtactttcct	4	>5.0	ttatttttagCTCTTTTGG	V
V	75	TTCTTCAAGgtatgggaac	5	2.5	acttttgtagCCCAACTGC	VI
VI	321	GGCTGCAAGgtgaatgaac	6	0.5	actattttagGTGAATTAG	VII
VII	118	ATTGCACAAgtatgcaaga	7	5.0	tttgttgcagTTCTCAGAA	VIII
VIII	172	CAAAAAGAGgtaaagcgaa	8	5.5	ttgcctttagTATGAAAAG	IX
IX	138	AATAATAATgtaagtcttt	9	>2.0		

Consensus $A_{64}G_{73}||g_{100}t_{100}.....a_{100}g_{100}||N$

3.2. Alternative Splicing in the Common Region.

Sequence comparisons of SLAP performed with BLAST search (Altschul 1990) indicated that it shares a significant sequence similarity with TOP_{AP}, a topographically graded antigen isolated from chick retina (Savitt 1995). Sequence similarity of 75% and 70% at nucleotide and amino acid level, respectively, suggests possible homology between the two cDNAs. The sequence alignment of TOP_{AP} with SLAP3 cDNA reveals two distinctive regions of sequence divergence (Figure 4). Two sequence gaps were observed in the 5' region (around nt 1760) and the 3' transmembrane region (nt 2590) of SLAP3. As the observed sequence gaps in SLAP could putatively be a result of alternative splicing of a primary nuclear SLAP transcript, RT-PCR analysis of rabbit cardiac RNA was performed with primers flanking the gaps (see Figure 4). Rabbit heart was chosen for analysis as it has been previously shown to express high levels of all SLAP isoforms. Rabbit cardiac total RNA was isolated by TriPure method and reverse transcribed. Primer pairs spanning the putative 5' and 3' transmembrane (TM) regions of divergence were synthesized (see Table 1 for primer sequence) and used in PCR analysis. Figure 5 displays the results of RT-PCR analysis of rabbit cardiac RNA with respective controls electrophoresed through 2% agarose gel and stained with Ethydium bromide. The regions of SLAP amplified by PCR is indicated at the top of the panel. The figure demonstrates that rabbit heart generates two variants in the 5' and TM regions, suggestive of alternative splicing. The two fragments were subcloned into pBlueScript KS plasmid and sequenced. Sequence analysis indicates that the 5' and TM higher molecular size SLAP variants resulted from splicing-in of novel in-frame putative exons of 142 and 90 nt, respectively.

Figure 4. Sequence Divergence Between SLAP3 and TOP_{AP} cDNAs.

Sequence alignment of the rabbit cardiac SLAP3 and chick retinal TOP_{AP} cDNA reveals two regions of sequence divergence, despite the overall nucleotide identities of 75%. The heterogeneity results due to presence of sequence gaps (*single underlined*) in the 5' (Panel A) and the 3' regions (panel B) of SLAP that may perhaps be generated by alternative splicing. Positions of primers utilized for PCR analysis that span the respective regions of divergence are denoted by *double underlined* sequences. The nucleotide positions given are relative to the SLAP3 and TOP_{AP} cDNA clones.

A)

```
TOP-AP AAGCAGCGACGACACTACGGATGCCCAAATGGATGACCAAGATCTAAATGAACCTATTGCTAAAGT        83
       :::::: ::::::::::::::: ::::::::::::::: ::::: :: :::::: :: ::::::::::
SLAP3  AAGCAGTGACGACACTACGGACGCCCAAATGGATGAGCAAGACCTGAATGAATCTCTTGCTAAAGTGTCC 1750

TOP-AP         AGCTCTTCTGAAAGATGAACTGCAGGGTGCACAATCAGAGACTGAGGCTAAGCAAGAAATTC  145
               :::::::
SLAP3  CTATTAAAAGCTCTT                                                       1765

TOP-AP AGCAGCTGCACAAGGAGCTGATTGAAGCCCAAGAGCTAGCTAGAACAAGTAAACAAAAATGCTTTGAACT  215

SLAP3                                                                       1765

TOP-AP TCAAGCGCTGTTGGAAGAAGAGAGAAGAGCATATAGAGTGCAAGTTGAAGAATCTAACAAGCAAATAAAT   2
                  :::::::::::: :::: ::: ::: ::   :::::::: ::::: :  :: :::::: :
SLAP3             TTGGAAGAAGAAAGAAAAGCCTATCGAAATCAAGTTGAGGAATCCAGTAAACAAATACAG 1825

TOP-AP GTTCTGCAAGCTCAGTTGCAGAGGTTACAGGAAGATATTGAGAATCTTCGTGAGGAGAAGGAGAGTGAAA  355
       ::::: ::::: ::  ::::::::::::::    :: :::::::::::: :: :::::::::::: : :::::
SLAP3  GTTCTTCAAGCCCAACTGCAGAGGTTACACATGGACATTGAGAATCTCCGGGAGGAGAAGGACAATGAAA 1895

TOP-AP TTTCTAGCACTCGAAACGAACTAGTCAGTGCTCAGAATGAGATTCTGTCACTTCAACAAGTAGCAGAAAA  425
       :  : :::::: :: : ::: :  : ::::: :   :::: ::: ::   ::::: :::: ::::::::::
SLAP3  TCACAAGCACTAGAGATGAATTGCTTAGTGCCCGAGATGAAATTTTGCTCCTTCATCAAGCAGCAGAAAA 1965
```

B)

```
TOP-AP CTGAAGGCGAAGTATGAGATGGCTGAACAAGAAAAGCAGTCAATCACAGAAGAGCTTAAACAGTGTAAAG 1006
       ::::::  ::::: ::: ::: :::: :: :::::::: :::::::::::: ::::: ::::: ::::::::
SLAP3  CTGAAGTTGAAGTTTGAAATGACTGAGCAGGAAAAGCAATCAATCACAGATGAGCTCAAACAATGTAAAG 2546

TOP-AP AAAACTTGAAGCTGCTGCAAGAAAAAGGAAAC       AACCCTTCCATATTACAACCCGTCCCAGCCG 1069
       : ::: :::::::::: ::::: ::::::::       :::::::  :
SLAP3  ACAACCTGAAGCTGCTCCAAGAGAAAGGAAATAATAATAAACCCTGGCCC                     2596

TOP-AP TATTCATCGGCCTAATCCTGGCTTTCCTGTATTGGTGTTACGGCCCATTGTGGTAGCGAAAGAGACAATG 1139

SLAP3                                                                       2596

TOP-AP GCCTTGGATGCCTGTGATGGCAGCTTTGGTTGCTGTGACAGCCGTGGTGCTGTACCCAGGCCTAA   CC 1206
            ::::::::  :: :::: ::  :::::::: ::::::::: : ::::::::            ::
SLAP3       TGGATGCCCATGTTGGCTGCCCTGGTTGCGGTGACAGCCATCGTGCTGTATGTGCCAGGTCTGGCC 2662

TOP-AP AGAGCTTCTCCACGAGAACTGTTGTTGAATCCATACACCGTCCTCCCTTTAGAAGCTGGCAACATTCATA 1276
       ::::::::::::  ::::    :: :::: ::: ::::::::::::::::: :::::::::::: ::  : :
SLAP3  AGAGCTTCTCCGTGAGAGTGTTTCTTGAGTCCGTACACCGTCCTCCCTCTAGAAGCTGGCATCACACTCA 2732

TOP-AP TACTGAGGGAAAACAGATTAATTC TCTTCCTTTTTTTGTTGTTTTCTTTTTTTTTTTTTTTTACCTCTT  1344
       : ::: ::::::::          :  ::::::::::::                              :::::::
SLAP3  TGCTG GGGAAAAACAGAACCATTTTCTTCCTTTTTT                               ACCTCTTA 2776

TOP-AP                    AATACAGCACAGCTCTGCGTGAGAACAGCAGTAGGGTCATTTGCTTTAAACT 1396
                          :::::: :                    ::::::::: :::::::::: :
SLAP3  AAACAACAGAAGTGCAAGAATACAACT                     GTAGGGTCA TTGCTTTAAATT 2824

TOP-AP GTATAAAATGTATCTGTCTATAAAGAGGGAATAAAATTGTGATTCATCA TACTGTGAGCAATATTTTTG 1465
        :::::::::::::::::: ::::::::  :::::::::::: :      :::::: :::::::  ::::
SLAP3  ATATAAAATGTATCTGTCTGTAAAGAGGATATAAAATTGTGACTTTATTCTACTGTAAGCAATAA TTTG 2893
```

Note:

1. Single underlined-bold print: regions of divergence.
2. Double underlined sequence: location of PCR primers.
3. Nucleotide positions given relative to TOP_{AP} and SLAP3 cDNAs.

Figure 5. Demonstration of 5' and TM Alternative Variants.

One μg of rabbit cardiac RNA was used for the first strand synthesis. PCR analysis of the 5' and TM regions of SLAP was performed with 5'.F and 5'.R, and TM.F and TM.R primers, respectively (see Table 1 for primer sequence). The PCR product were electrophoresed through 1% agarose gel and the DNA was visualized with Ethydium bromide staining. Top of the panel indicates the region of SLAP that was analyzed. Lanes 'H' represent rabbit heart experimental lanes, whereas the '+' denotes cloned SLAP1 cDNA positive controls lacking alternative exons. RT-PCR revealed expression of two variants in the 5' and TM regions. The novel variants were subcloned and sequenced.

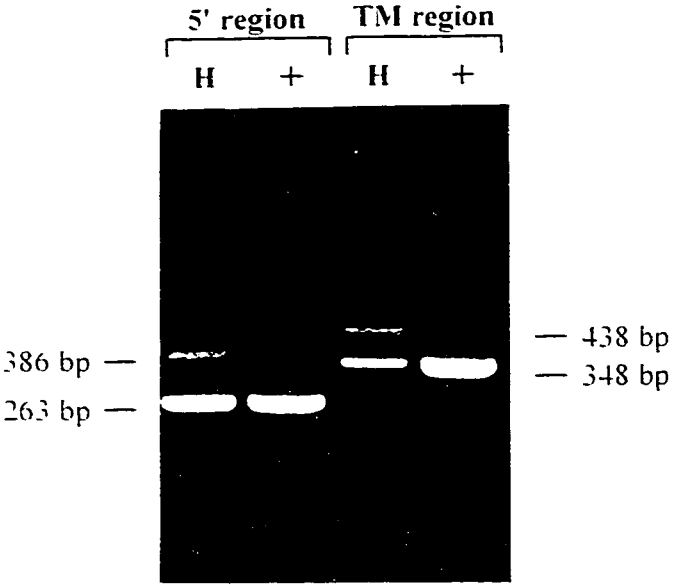

Note: 1. H : Heart experimental lane

2. + : corresponding SLAP1 positive controls

A sequence alignment of rabbit cardiac SLAP variants with chick retinal TOP_{AP} cDNA is shown in Figure 6 and reveals that the sequence of the putative alternative exons, their length and alternative splicing sites are identical in TOP_{AP} and SLAP cDNAs. The sequence similarities of the putative alternative 5' and TM exons with TOP_{AP} cDNA are 90% and 88% at amino acid level, respectively.

In order to determine whether retina expresses a splice variant without the alternative exons, in addition to TOP_{AP}-like variant, adult rat retina RNA was reverse transcribed and PCR amplified with primers specific for the 5' alternative region of rabbit SLAP (see Table 2). The RT-PCR analysis revealed that as in rabbit heart, rat retina also expresses two variants. Panel (a) of Figure 7 displays a nucleotide sequence alignment of rat retinal and rabbit cardiac SLAP variants with chick retina TOP_{AP} cDNA. The length of the alternative 5' exon and splicing site are identical to that of rabbit and chicken. The rat retinal 5' alternative exon shares 89% and 80% sequence identities with the rabbit at nucleotide and amino acid levels, respectively, as well as, 78% and 72% identity with chick retinal TOP_{AP}. The RT-PCR approach to amplify 5' alternative region from more evolutionarly distant species (salamander and trout) was unsuccessful as the sequences were perhaps too distant. Moreover, RT-PCR based approach for amplification of the TM region variants from rat also failed. Instead a human cardiac muscle cDNA library was screened with AvaI-HindIII (1607-1926) restriction fragment of SLAP3. Screening of $1x10^6$ pfu yielded three positive clones Hum-H1, Hum-H2 and Hum-H3. Direct sequencing revealed that Hum-H1 included alternatively spliced TM exon, similar to rabbit heart and chick retinal TOP_{AP}. The sequence alignment of human and rabbit cardiac

Figure 6. Alignment of 5' and TM alternative variants of SLAP with TOP_{AP}.

Sequence alignment of rabbit cardiac SLAP variants (SLAP and RAB-H) with chick retinal TOP_{AP} is shown. The alignment indicates that the sequence gaps observed in the 5' and the TM region are a result of splicing in of a 142 nt (Ai) and 90 nt sequences (Aii) (*underlined*), respectively. Alignment of predicted amino acid sequences is depicted in panel B. The nucleotide and amino acid identities are denoted by *asterisks*.

A)

i) 5' region.

```
SLAP    TATTAAAAG
RAB-H   TATTAAAAGATGACTTGCAGGGTGCACAGTCAGAAACTGAGGCAAAACAAGAAATTCAGCATCTTCGCAAGGAATTGA
TOP-AP TTCTGAAAGATGAACTGCAGGGTGCACAATCAGAGACTGAGGCTAAGCAAGAAATTCAGCAGCTGCACAAGGAGCTGA
               ****  ************* ***** ******** ** ************** ** * ******  ***

SLAP                                                                    CTCTTTTGGAAGAAGAAAGAAAAG
RAB-H   TCGAAGCCCAGGAGCTAGCTAGAGCAAGTAAACAAAAATGCTTTGAACTTCAAGCTCTTTTGGAAGAAGAAAGAAAAG
TOP-AP TTGAAGCCCAAGAGCTAGCTAGAACAAGTAAACAAAAATGCTTTGAACTTCAAGCGCTGTTGGAAGAAGAGAGAAGAG
       * ******** ************ ********************************
```

ii) TM region.

```
SLAP    AATAAT
RAB-H   AATAATCCTTCCATATTACAACCCGTCCCAGCCGTATTCATCGGCCTATTCCTGGCTTTCCTGTTTTGGTGTTTCGGT
TOP-AP AAC   CCTTCCATATTACAACCCGTCCCAGCCGTATTCATCGGCCTAATCCTGGCTTTCCTGTATTGGTGTTACGGC
             ****************************************** ************** ******** ***

SLAP                        AAACCCTGGCCCTGGATGCCCATGTTGGCTGCCCTGGTTGCGGTGACAGCCATCGTGCTG
RAB-H   CCATTGTGGTAGAGAAAGAAACCCTGGCCCTGGATGCCCATGTTGGCTGCCCTGGTTGCGGTGACAGCCATCGTGCTG
TOP-AP CCATTGTGGTAGCGAAAGAGACAATGGCCTTGGATGCCTGTGATGGCAGCTTTGGTTGCTGTGACAGCCGTGGTGCTG
       ************ *****

SLAP    TATGTGCCAGGTCTGGCCAGAGCTTCTCCGTGAGAG
RAB-H   TATGTGCCAGGTCTGGCCAGAGCTTCTCCGTGAGAG
TOP-AP GTAC  CCAGGCCTAACCAGAGCTTCTCCACGAGAA
```

B)

i) 5' region.

```
                        ALTERNATIVE 5' EXON
SLAP    AKVSLLK-----------------------------------------ALLEEER
RAB-H   AKVSLLKDDLQGAQSETEAKQEIQHLRKELIEAQELARASKQKCFELQALLEEER
TOP-AP AKVALLKDELQGAQSETEAKQEIQQLHKELIEAQELARTSKQKCFELQALLEEER
             * *************** * *********** *********
```

ii) TM region.

```
                          TM-1 EXON                        TM-2 EXON
SLAP     QEKGNNN-------------------------------KPWPWMPMLAALVAVTAIVLYVPGLARASP.ECF
RAB-H    QEKGNNNPSILQPVPAVFIGLFLAFLFWCFGPLW^RKKPWPWMPMLAALVAVTAIVLYVPGLARASP^ECF
TOP-AP   QEKGNN-PSILQPVPAVFIGLILAFLYWCYGPLW^RKRQWPWMPVMAALVAVTAVVLY-PGLTRASPRELI
               ************** **** ** *******  *****  ******** *** *** ****
```

Note 1. * : homology identities
2. bold-underlined: alternative exons
3. shadow or ^ : STOP codons

Figure 7. Conservation of Alternative Splicing in the 5' and TM regions of SLAP among species.

RT-PCR and cDNA library screening approaches were utilized to isolate the 5' and TM alternative regions of SLAP from rat retina and human heart. Sequence gaps are denoted by *dashes*. Panel A depicts sequence alignment of rabbit cardiac (SLAP1 and Rab-H) and rat retinal variants (Rat-R_1 and Rat-R_2) with chick retinal TOP_{AP}. The alignment demonstrates conservation of the alternative splicing of the 5' exon (*underlined*) in rabbit, rat and chicken. Panel B on the other hand, demonstrates sequence alignment of the TM region rabbit cardiac variants (SLAP1 and Rab-H) with human cardiac SLAP (Hum-H1) and rat retinal TOP_{AP}. The alternative spicing of TM exon is thus conserved between rabbit, human and chick. Interestingly, the TM alternative exon encodes highly hydrophobic polypeptide and contains an in-frame chain termination codon (denoted by '^') . The alternative exon thus might serve as an alternative membrane anchor for SLAPs.

A)

Alternative 5' Exon

```
SLAP1    VSLLK----------ALLEEERKA
Rab-H    VSLLKDDLQGAQSETEAKQEIQHLRKELIEAQELARASKQKCFELQALLEEERKA
Rat-R1   VSLLK----------ALLEEERKA
Rat-R2   VSLLKDDLQGTQAETEAKQDTQHLRKELVEAQELAGASKQKCFDLQALLEEERKA
TOP-AP   VALLKDELQGAQSETEAKQEIQQLHKELIEAQELARTSKQKCFELQALLEEERRA
```

B)

```
                    Alternative TM-1 EXON                    Constitutive TM-2 EXON
SLAP     QEKGNNN----------KPWPWMPMLAALVAVTAIVLYVPGLARASP-ECF
Rab-H    QEKGNNNPSILQPVPAVFIGLFLAFLFWCFGPLW^RKKPWPWMPMLAALVAVTAIVLYVPGLARASP^ECF
Hum-H1   REKGNN-PSILQPVPAVFIGLFLAFLFWCFGPLW^RKKPWPWMPMLAALVAVTAIVLYVPGLARASP^ERS
TOP-AP   QEKGNN-PSILQPVPAVFIGLILAFLYWCYGPLW^RKRQWPWMPVMAALVAVTAVVLY-PGLTRASPRELI
```

Note: 1.bold-underlined: alternative exons

2.shadow or ^: STOP codons

alternative TM regions of SLAP with chick retinal TOP_{AP} is shown in Figure 7b. Human alternative TM exon is of identical length and shares the same splice-in site as rabbit alternative variant and TOP_{AP} cDNA. Alternative human TM exon shares a 100% identity with rabbit at both nt and A.A. level, as well as 94% and 88% sequence identity with TOP_{AP}, respectively.

Based on the sequence alignment of alternative exons, their length, as well as common site of divergence, a model of putative genomic organization generating alternatively spliced variants was proposed. The model is depicted in Figure 8, where panel 8a predicts skipping or inclusion of 5' alternative exon to produce two 5' variants observed in rabbit heart and rat retina, as well as an alternative variant in the TOP_{AP}. Panel 8b demonstrates a model that generates two variants containing either of the mutually exclusive transmembrane domains, as a result of skipping or inclusion of an alternative transmembrane domain containing an alternative stop codon. The putative models predicts canonic donor and acceptor splice sites in the alternative exons, based on the exon-exon boundaries determined by genomic organization studies of SLAP gene.

Figure 8. Genomic organization model of 5' and TM alternative Exons.

A graphical model of the genomic organization of the alternatively spliced 5' and TM exons of the SLAP gene was proposed based on the conservation of alternative splicing among the species (rabbit, rat, human and chick). The model predicts that the 5' alternative exon is either included or skipped with no change of the open reading frame. Splicing of the alternative TM exon (TM1), on the other hand introduces an in-frame STOP codon, that results in an alternative carboxyl terminal of SLAP. The expression of the TM exons is therefore mutually exclusive.

skipped exon

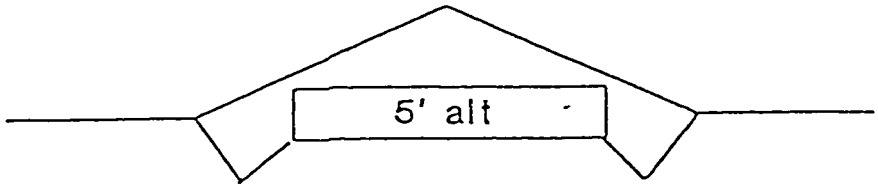

mutually exclusive exons

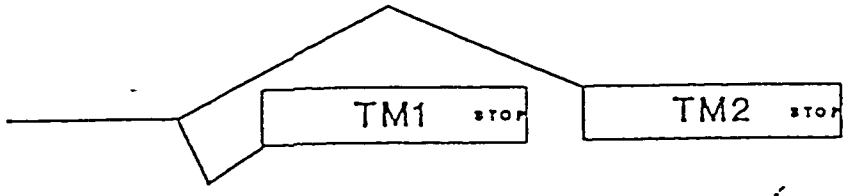

3.3. Alternative Splicing of SLAP gene in Other Regions.

The nucleotide alignment of SLAP2 and SLAP3 cDNA clones with SEQAIDII program revealed a 63 nt sequence gap in SLAP2. Moreover, a previously isolated human SLAP clone (Hum-H1) was found to contain, in addition to the aforementioned 63 nt sequence, a novel in-frame 51 nt fragment located immediately 5' of the 63 nt sequence. Figure 9 depicts nucleotide and amino acid sequence alignments of Hum-H1, SLAP2 and SLAP3 clones. The sequence alignment strongly suggests that two tandem fragments of 51 and 63 nt might result due to alternative splicing of the SLAP primary transcript, thus generating identified SLAP variants. Based on the sequence alignment a putative genomic organization model of 51 and 63 nt putative exons was proposed (see Figure 10), where two tandem alternatively spliced exons are independently spliced generating four distinct variants: the first with both alternative fragments, the second with none and, the third and the forth with either of the two fragments. The SLAP cDNA clones (SLAP2, SLAP3 and Hum-H1) represent three of four theoretically predicted variants.

Figure 9. Alternative splicing of 51 and 63 nt exons.

Sequence alignment of two rabbit cardiac SLAP isoforms (SLAP2 and SLAP3) with human cardiac (Hum-H1) cDNA reveals two sequence gaps of 51 nt (*underlined*) and 63 nt (*double underlined*), that is indicative of alternative splicing. Sequence gaps are denoted by *dashes* and sequence identities by *asterisks*. Panel A depicts nucleotide alignment whereas panel B an alignment of deduced protein sequence.

A)

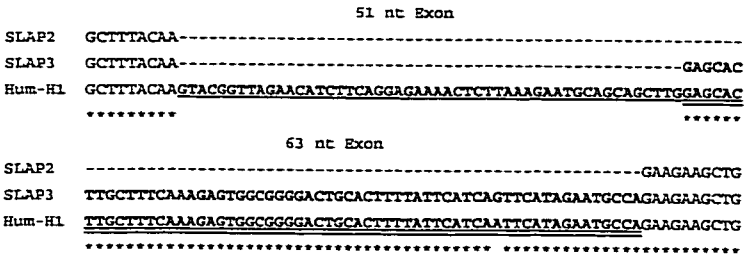

B)

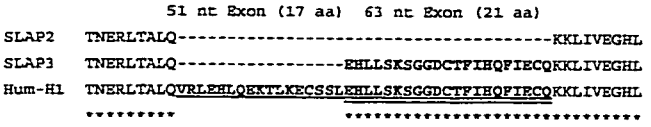

Note: **Bold-underlined**: alternative exons

* : identity homology

Figure 10. Genomic organization of 51 and 63 nt alternative exons.

A genomic organization model of the 51 and 63 nt alternative exons was proposed based on the sequence alignment of the rabbit cardiac isoforms (SLAP2 and SLAP3) with human cardiac variant (Hum-H1). The model predicts generation of four isoforms by independent splicing of the two exons. The first isoform would contain both exons (Hum-H1-like), the second only 51 nt exon, the third only the 63 nt exon (SLAP3-like) and finally fourth variant none of the two exons (SLAP2-like).

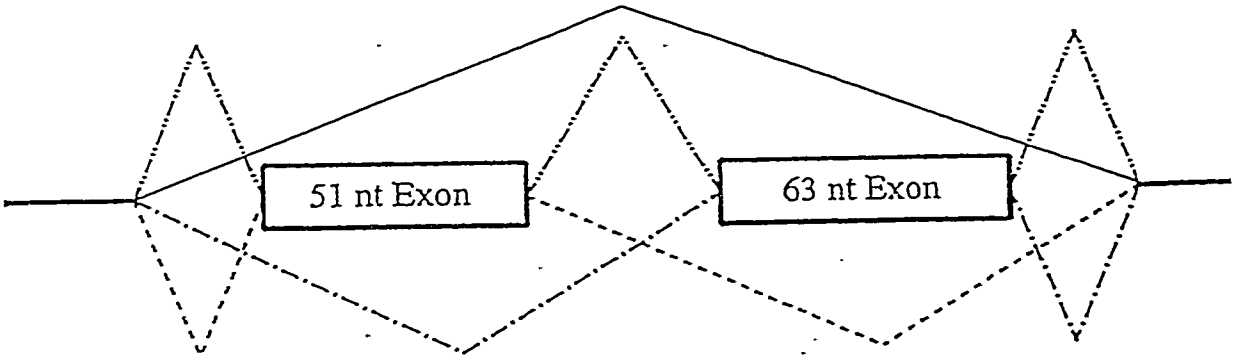

—·—·— Both exons

—— No exons

—·—·— Only 63 nt exon

- - - - Only 51 nt exon

3.4. Tissue-specific Expression of SLAP Alternative Exons.

In order to determine whether the expression of alternative exons is tissue specific, RNA from various rabbit tissues was harvested and analyzed by RT-PCR with specific primers for each of the alternative regions of SLAP (see Table 1). The tissues analyzed included heart, left and right ventricles, atria, heart septum, brain, liver, lungs, kidneys, pancreas, spleen, ovaries, soleus and fast-twitch muscle.

a) Expression of 51 and 63 nt Alternative Exons.

The results of RT-PCR analysis using the SLAP3.F and SLAP3.R primers for amplification of 51 nt and 63 nt alternative exons is shown in Figure 11a. Results reveals that all adult rabbit tissues examined express three alternative variants: Hum-H1 (top), SLAP3 (middle) and SLAP2 (bottom) with either both, one or none of the alternatively spliced exons. However, the three variants appear to be expressed in different proportions. The SLAP2-like variant (without either of 51 and 63 nt alternative exons) appears to be a predominant isoform, while SLAP3-like isoform (with 63 nt exon) exhibits an intermediate expression and the Hum-H1-like isoform (with both alternative exons) the lowest level. These results are qualitative as 1.0 μg of total RNA was used in each sample for RT reaction, without normalization of SLAP mRNA levels.

Figure 11. Tissue-specific Expression of SLAP Alternative Exon.

RT-PCR was used to amplify the alternative regions of SLAP from various rabbit tissues in order to examine the tissue-specific expression of the SLAP variants. One μg of total rabbit RNA was reverse transcribed and the respective alternative regions were amplified by PCR with the corresponding primers (see Table 1). Panel A depicts tissue-specific expression of the 51 and 63 nt exons. Cloned cDNAs Hum-H1, SLAP3 and SLAP2 are used as positive controls, where Hum-H1 clone contains both the 51 and 63 nt exons, SLAP3 only 63 nt exon, and SLAP2 neither of the two exons. Panel B demonstrates tissue-specific expression of the 5' alternative exon. The positive controls include: '+ve alt' containing 5 alternative exon and 'SLAP1' without the 5' exon. The tissue specific-expression of the TM alternative exon is summarized in panel C. The '+ve alt' positive control is representative of variants containing the TM alternative exon, whereas the '+ve SLAP1' lacks the alternative TM exon.

A)

Heart
L vent
R vent
Septum
Atria
Soleus
FT
Brain
Kidney
Lung
Pancreas
Spleen
Liver
Ovary
-ve
+ve Hum-Sk
+ve SLAP3
+ve SLAP2
219
168
105

B)

Heart
L vent
R vent
Septum
Atria
Soleus
FT
Brain
Kidney
Lung
Pancreas
Spleen
Liver
Ovary
-ve
+ve alt
+ve SLAP1
386
263

C)

Heart
L vent
R vent
Septum
Atria
Soleus
FT
Brain
Kidney
Lung
Pancreas
Spleen
Liver
Ovary
-ve
+ve alt
+ve SLAP1
438
348

b) Expression of SLAP 5' Alternative Exon.

The results of RT-PCR analysis of tissue-specific expression of SLAP1 5' alternative exon are summarized in Figure 11b. Results reveal that all of the tissues examined express two variants: a higher molecular size band including the 5' alternative exon and a lower band without the alternative exon, except for right ventricle and atria, where the reaction has failed. In heart, soleus, fast-twitch muscle and lungs the lower molecular size isoform (without the 5' alternative exon) is more predominant. On the other hand, kidneys, pancreas, spleen, liver and ovaries express preferentially the higher molecular size isoform including the alternative 5' exon. Brain is the only tissue where the expression of both isoforms appears to be similar.

c) Expression of SLAP TM Alternative Exon.

Analysis of the tissue-specific expression pattern of the TM alternative exon also utilized the RT-PCR approach. The results of the analysis are shown in Figure 11c. The data indicate that all of the tissues examined express two variants, with and without the alternative TM exon. However these variants are expressed at different levels. Heart, the left and right ventricles, septum, atria and pancreas demonstrate a higher expression of the lower molecular size isoform (without the alternative TM exon), whereas, kidney, lung, spleen, liver and ovaries preferentially express the higher molecular size isoform (with the alternative TM exon). None of the tissues examined appear to express exclusively any of the two alternatively spliced transcripts.

3.5. Developmental Expression of 5' Alternative Exon.

In order to determine whether the alternatively spliced variants of SLAPs were expressed in a developmentally regulated manner three distinct stages of rat development: fetal (day 18 of gestation), neonatal and adult, was examined by RT-PCR analysis.

The results of a developmental analysis of the 5' alternative exon are summarized in Figure 12. Panel 12a corresponds to fetal and panels 12b to neonatal and adult stages of development. A comparison of expression levels in brain and kidney during fetal and neonatal (pup) stages shows that there is an increase in the level of expression of a higher molecular size variant (with 5' alternative exon). On the other hand, transition from neonatal to adult stage of development demonstrates a decrease in expression of the higher molecular size variant in brain, lung and spleen.

The RT-PCR analysis of the TM variant expression in developing rat with rabbit SLAP primers was unsuccessful, as perhaps the rabbit based 3' UTR *TM.R* antisense primer shared low homology with rat 3' UTR.

Figure 12. Developmental expression of 5' alternative exon.

First-strand cDNA was amplified by PCR with primers 5'.F and 5'.R (see Table 2). RNA was harvested from rat tissues at fetal (day 18 of gestation), neonatal (day 4) and adult stages of development. PCR products were electrophoresed through 2% agarose gel and visualized by Ethydium bromide fluorescence. Rat retinal SLAP constructs containing the 5' alternative exon ('+ve alt') and lacking the alternative exon ('SLAP1-like') were used as positive controls. Panel A depicts tissue-specific expression of the 5' alternative variants in the fetal rat at the 18^{th} day of gestation. Panel B demonstrates the tissue-specific expression at the neonatal (day 4) and adult developmental stages.

A)

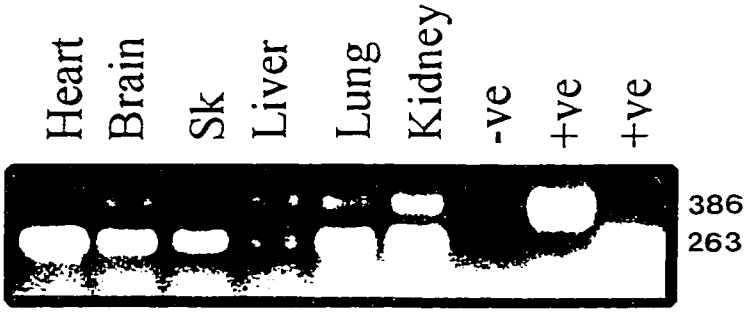
Heart
Brain
Sk
Liver
Lung
Kidney
-ve
+ve
+ve
386
263

B)

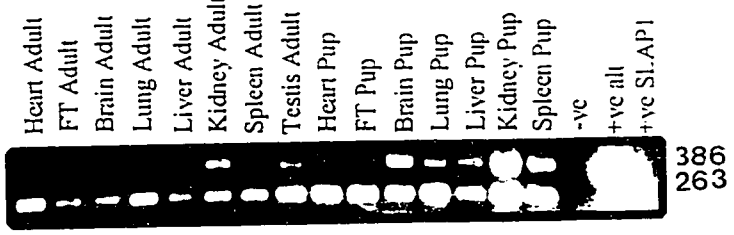
Heart Adult
FT Adult
Brain Adult
Lung Adult
Liver Adult
Kidney Adult
Spleen Adult
Testis Adult
Heart Pup
FT Pup
Brain Pup
Lung Pup
Liver Pup
Kidney Pup
Spleen Pup
-ve
+ve all
+ve SLAP1
386
263

3.6. Species Differences in Expression of 5' Alternative Exon.

The comparison of adult rat and rabbit expression pattern of the 5' alternative variants (compare Figures 11b and 12b) reveals that species-specific differences in expression of 5' alternative exon exist. The differences in expression pattern exist in heart, brain, kidney and spleen, whereas in lungs, liver and FT muscle the expression pattern was similar.

Rat heart expresses only one variant (without the 5' alternative exon), whereas rabbit heart expresses both. On the other hand, rat and rabbit brain express the two variants, while, rat preferentially the smaller (lacking the 5' alternative exon) and in rabbit both variants appear to be present in equal amounts. In rat kidney both variants are expressed in equal ratio, while in rabbit kidney the 5' alternative variant is expressed preferentially. Lastly, the spleen from rat and rabbit expresses both variants, with rat expressing predominantly the lower molecular size variant and rabbit the larger 5' alternative variant.

3.7. Complete Genomic Structure of the 3' end of SLAP Gene.

The RT-PCR analysis of rabbit heart RNA revealed that 5' and TM regions of SLAP are alternatively spliced (Figure 5 and 6). Moreover, the alternative splicing of these exons is conserved in rabbit, rat and human SLAPs, as well as the chick TOP_{AP}. Based on sequence alignment of the SLAP alternative variants, the putative genomic organization models predicting the presence of two alternatively (5' and TM) exons located between exons III and V, and IX and XI are proposed. In order to verify the putative model, the alternative exons had to be isolated in the genomic sequence.

Consequently, the previously isolated non-overlapping rabbit genomic clones R-2, R-13 and R-14 were screened by Southern Blot analysis with PCR-amplified alternative exon probes to isolate the alternative exon. However, this approach failed to isolate alternative exons indicative of their absence in these rabbit genomic clones. The rabbit genomic library was therefore re-screened with cDNA probes containing the alternative exons, however, no new clones were isolated in addition to previously characterized non-overlapping clones. Re-screening of the rabbit genomic library with PCR-generated alternative exon probes was also unsuccessful.

Screening of $0.5x10^6$ pfu of mouse genomic λDASHII library with *Sal1-EcoR1* fragment of SLAP3 cDNA (1-3117) yielded two positive clones (M-2 and M-3). Further analysis of mouse clones by Southern Blot with alternative exon probes revealed that M-3 and M-2 clones contained the 5' and TM alternative exons, respectively. In view of isolation of SLAP alternative 5' and TM exons from mouse, but not rabbit genomic library, it is indicative that available rabbit genomic library was not representative of the

entire 3' end of SLAP gene. The successful isolation of alternative exons from mouse genomic library may be attributed to differential library design. Mouse genomic DNA was prepared by partial restriction digestion with a frequent cutter (*Mbo1*), while rabbit genomic DNA with a rare cutter (*BamH1*). Moreover loss of clones during library amplification may also account for absence of alternative exons in the rabbit library.

Southern Blot analysis of the mouse genomic clones followed by subcloning and direct sequencing revealed that length of mouse exons and mouse exon-exon boundaries paralleled those elucidated in the rabbit. Table 3 contains a sequence alignment of rabbit and mouse intron-exon boundaries of the 3' end of the SLAP gene. The comparison demonstrates that the two species share identical genomic organization revealed by conservation of exon-exon boundaries, exon length and intron-exon junctions. This conservation strongly suggests that the splicing mechanism of SLAP is conserved between these two mammalian species.

TABLE 3. Comparison of genomic organization of rabbit and mouse SLAP genes.

Screening of rabbit and mouse genomic libraries for the SLAP gene followed by direct sequencing of the positive clones allowed to characterize SLAP exons and the respective intron-exon junctions in the two species. The summary of the comparison of the rabbit and mouse intron-exon junctions is presented below, where *R* denotes the rabbit and *M* the mouse SLAP gene. The exon sequence is presented in *upper-case* whereas introns are gives in *lower-case*. Conserved 'gt-ag' intron dinucleotides sequences are printed in ***bold***.

Intron	EXON	no.	Intron size (nt)	
	cagAGAAGCTGA..	I_R	60	..CTTGCAAAAGgtc
	tagAAAACCAGG..	II_R	81	..GACACTACGGgtg
	tagAAATCAGGC..	II_M	81	..GACACTACAGgtg
	aagACGCCCAAA..	III_R	60	..CTATTAAAAGgta
	tagACGCCCAGA..	III_M	60	..TAATTAAAAGgta
	...ATGACTTGC..	IV_R	123	..GAACTTCAAG...
	tagATGACTTAC..	IV_M	123	..GAACTTCAAGgtg
	tagCTCTTTTGG..	V_R	75	..GTTCTTCAAGgta
	tagCTCTTTTGG..	V_M	75	..GTTCTTCAAGgta
	tagCCCAACTGC..	VI_R	321	..AGGCTGCAAGgtg
	cagTCCAGCTGC	VI_M	321	..AGGTTGCAAGgta
	tagGTGAATTAG..	VII_R	118	..AATTGCACAAgta
	tagGTGAGCTGG	VII_M	118	..AATTGCACAAgta
	cagTTCTCAGAA..	$VIII_R$	172	..CAAAAAGAGgta
	tagTATGAAAAG..	IX_R	138	..AAATAATAATgta
	tagTATGAAAAG	IX_M	138	..AAATAATAATgta
	...CCTTCCATA..	X_R	90	..GTAGAGAAAG...
	cagCCCTCCATA..	X_M	90	..GTAGAGAAAGgta
	...AAACCCTGG..	XI_R	>90	..TCTCCGTGA.3'UTR
	cagAAACCCTGG..	XI_M	>90	..TCTCCATGA.3'UTR

TGA/TAG stop codons
R: rabbit
M: mouse

The complete exon map of 3' end of SLAP gene, based on the rabbit and mouse genomic data is displayed in Figure 13. The genomic organization reveals 11 exons ranging in size from 60 nt to 321 nt. Exons IV and X represent 5' and TM alternative exons, respectively. Exons VII and VIII, on the other hand, contain the leucine zipper motifs, while the two mutually exclusive transmembrane anchors are located in alternative exon X and constitutive exon XI, respectively. The intron-exon junctions of 3' end of SLAP gene have been identified by direct sequencing of the rabbit and mouse genomic subclones and summarized in Table 4. All of the identified constitutive and alternative SLAP introns started and ended with 'gt' and 'ag', respectively, thus conforming to the canonic GT-AG rule of intron acceptor and donor sites.

Figure 13. Exon-exon boundaries of the 3' End of the SLAP Gene.

A schematic diagram depicts exon-exon boundaries of the 3' end of the SLAP gene common to all SLAP isoforms. The *open boxes* represent constitutively expressed exons while the *shaded boxes* (exons IV and X) represent alternatively spliced exons 5' and TM, respectively. The numbers above the respective exons denote exon length while the nucleotide ranges below the exons represent locations of the respective exons in the cloned SLAP3 cDNA. The bottom panel is a schematic depicting rabbit and mouse genomic clones spanning the 3' end of the SLAP gene.

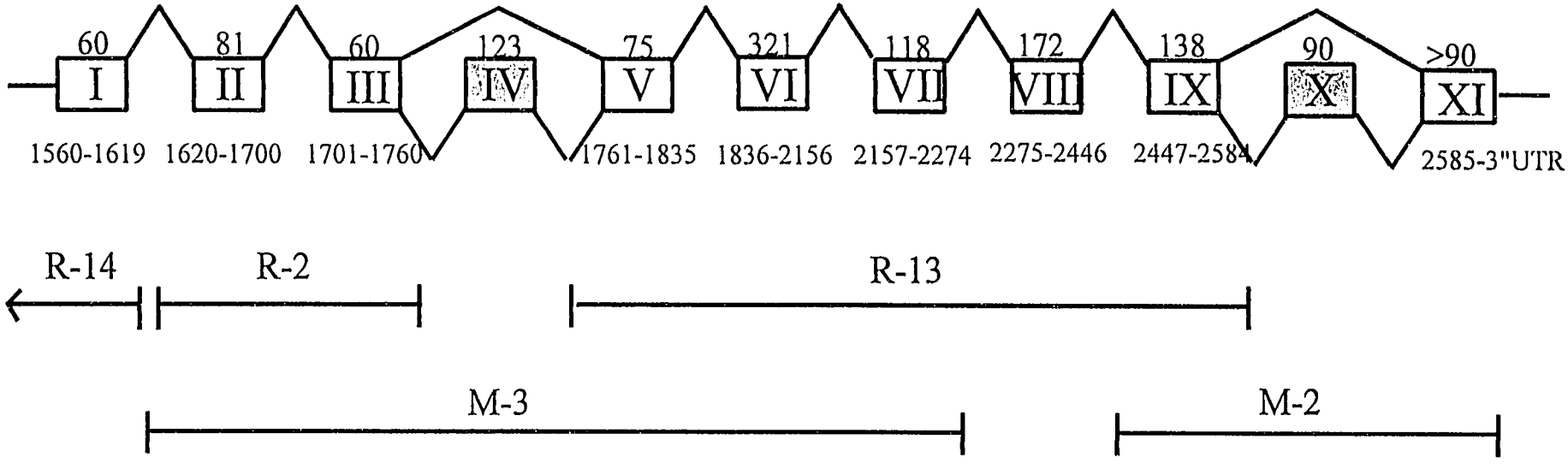
60
81
60
123
75
321
118
172
138
90
>90
I
II
III
IV
V
VI
VII
VIII
IX
X
XI
1560-1619
1620-1700
1701-1760
1761-1835
1836-2156
2157-2274
2275-2446
2447-2584
2585-3"UTR
R-14
R-2
R-13
M-3
M-2

TABLE 4. Complete Compendium of Intron-Exon Junctions of the 3' End of the SLAP gene.

Direct sequencing of the rabbit and mouse genomic DNA allowed to elucidate the complete intron-exon map of the 3' end of the SLAP gene that comprises the entire coding region of the SLAP1 isoform. The exons are denoted in the *upper-case* and the introns by the *lower-case*. *Roman* and *arabic* numerals represent exons and introns, respectively. The intron 5' and 3' dinucleotide consensus sequences are given in ***bold***. The in-frame stop codons (*shaded)* of the mutually exclusive transmembrane domains are located in exons X and XI. The sequences derived from the mouse are denoted with *asterisks*.

Exon No.	Exon Size bp	Exon	Intron No.	Intron Size kb	Intron Class	Exon	Exon No.
-	--	.....	1	>3.5	1	tctttggcagAGAAGCTGA	I
I	60	TTGCAAAAGgtcgttttct	2	>2.0	1	ctctctgtagAAAACCAGG	II
II	81	ACACTACGGgtgagtttta	3	0.2	1	cctctcgaagACGCCCAAA	III
III	60	TATTAAAAGgtactttcct	4	>5.0	1	tttttgtcagATGACTTGC	IV
IV	123	AACTTCAAGgtgagatgaa*	5	>3.0	1	ttatttttagCTCTTTTGG	V
V	75	TTCTTCAAGgtatgggaac	6	2.5	1	acttttgtagCCCAACTGC	VI
VI	321	GGCTGCAAGgtgaatgaac	7	0.5	1	actattttagGTGAATTAG	VII
VII	118	ATTGCACAAgtatgcaaga	8	5.0	2	tttgttgcagTTCTCAGAA	VIII
VIII	172	CAAAAAGAGgtaaagcgaa	9	5.5	0	ttgcctttagTATGAAAAG	IX
IX	138	AATAATAATgtaagtcttt	10	>2.0	0	ccttcttcagCCCTCCATA*	X
X	90	TAGAGAAAGgtacaagcac*	11	>1.6	0	ttccacacagAAACCCTGG*	XI
XI	>90	TCTCCATGA.....*	12			....3' UTR	
Consensus		$A_{64}G_{73}\|\|g_{100}t_{100}$.....$a_{100}g_{100}\|\|N$					

TAG/TGA stop codons
* based on mouse genomic sequence

DISCUSSION

Isolation of genes involved in the control of cardiac E-C coupling reveals a plethora of molecular diversity generated by multigene families, utilization of alternative promoters and alternative splicing mechanisms. Previous investigation into the characterization of a putative Ca^{2+}-binding protein of the sarcolemma led to the isolation of cDNAs encoding a novel sarcolemmal associated protein (SLAP). SLAPs are a family of acidic amphipathic alpha-helical proteins associated with the membrane. Although three SLAP isoforms were identified and shown to be expressed in a tissue-specific pattern, the SLAP family is encoded by a single gene mapped to human chromosome 3p14.3-21.2. The deduced protein structure of SLAPs predicts an extended coiled-coil with two leucine zippers and a carboxyl terminal transmembrane domain. In light of SLAP heterogeneity the molecular mechanisms that give rise to the multiple SLAP isoforms had to be investigated.

Research in this study centered on the determination of the genomic organization of the 3' end of the SLAP gene, as well as, demonstration of alternative splicing of the SLAP primary transcript.

The results demonstrate that the 3' end of the SLAP gene, corresponding to the common region of SLAP1, SLAP2 and SLAP3 isoforms (1560-2675), spans over 35 kb of genomic DNA (Figure 14). The 3' region of the SLAP gene is composed of 11 exons ranging in size from 60 to 321 bp. These exons comprise the entire coding region of SLAP1 isoform. Exons IV and X were found to be alternatively spliced, whereas the

Figure 14. Exon composition of SLAP peptide isoforms.

The figure depicts exon composition of SLAP protein isoforms, where *solid boxes* represent mapped exons of SLAP gene while *dotted boxes* denote unmapped exons in the 5' end of the SLAP gene. The alternatively spliced exons are depicted as *shaded boxes*. All SLAP isoforms contain leucine zipper motifs (LZ) and mutually exclusive trandmembrane domains (TM_1 and TM_2).

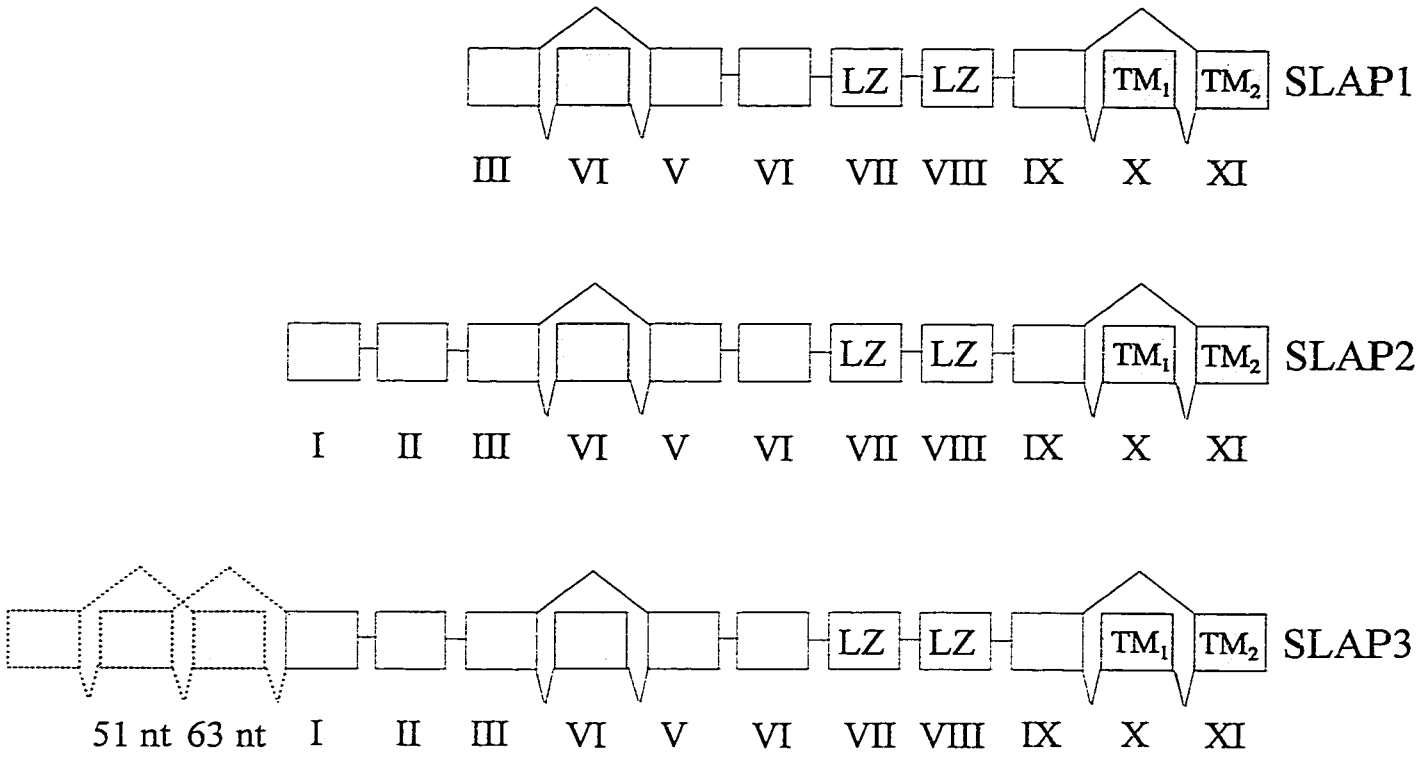

Mapped exons

Unmapped exons

Alternatively Spliced Exons

LZ Leucine Zipper

TM Transmembrane Domains

other exons are expressed constitutively. Exons I and II represent the coding exons of SLAP2 and SLAP3 isoforms, while in SLAP1 they are untranslated. Exon III contains the first methionine of SLAP1 isoform. Exon VII and VIII, both contain predicted leucine zippers, whereas exon VIII in addition contains a glutamate stretch composed of six glutamate heptad repeats. Exon XI encodes a carboxyl-terminus containing an in-frame stop codon and the 3' untranslated region. On the other hand, the alternatively spliced exon X encodes an alternative carboxyl-terminus with an alternative stop codon. Since exons X and XI are both predicted to encode a C-terminal membrane anchor, the alternative utilization of exon X results in generation of a SLAP variant with a different transmembrane domain (discussed in more detail below).

Sizes of the SLAP introns range from 0.2 to 5.5 kb. All of the identified introns begin with a 'gt' and end with an 'ag', strictly conforming to canonical 'gt-ag' rule of intron donor and acceptor sites (Mount 1982). Introns 1, 2, 3, 4, 5, 6 and 7 represent class 1 introns, where each intron interrupts the coding sequence between the first and the second bases of the codon. Intron 8 belongs to class 2 (it interrupts the second and the third bases of the codon), whereas introns 9, 10 and 11 are class 0 (the intron occurs between codons). As introns 1 through 7 and 9 through 11 represent introns of the same class, the open reading frames (ORFs) are good candidates for exon shuffling. Moreover, as the alternative exons IV and X are flanked on either side by class 1 or class 0 introns, respectively, the alternative splicing, therefore results in a conservation of the open reading frame of SLAP.

The study also demonstrates that SLAP isoform heterogeneity arising due to the alternative usage of the N-terminal is further diversified by the alternative splicing of a SLAP primary transcript in three distinct regions. In the SLAP2/3 region (1386-1560), two alternatively spliced putative 'cassette' exons of 51 and 63 nt were identified. The 51 nt exon contains putative consensus phosphorylation sites for protein kinase C (PKC) and casein kinase II (CKII), whereas the 63 nt exon has only a CKII phosphorylation site. Family of PKC's is implicated in a number of processes such as growth, differentiation and cytokine release. CKII, on the other hand represents ubiquitous kinase localized to the nucleus and cytoplasm, that phosphorylates multiple substrates functioning in control of cell division and in signal transduction (Allende 1995 and Pinna 1997). The 51 nt exon is predicted to form extended alpha-helix thus conforming to the overall deduced structure of SLAP. The 63 nt exon, on the other hand, is predicted to encode extended beta-sheet and secondary structure turns, as determined using SEQAID protein structure prediction program (University of Kansas). The putative PKC and CKII phosphorylation sites introduced by alternative splicing are not , however, unique as SLAP polypeptide contains numerous putative phosphorylation sites for casein kinase II (20 sites) and protein kinase C (12 sites). Although the effects of inclusion of the putative phosphorylation sites and the predicted changes in the secondary structures on the SLAP function remain unclear, a conservation of the alternative splicing of the 51 and the 63 nt exons in human and rabbit is indicative of a functional role of the 51 and 63 nt exons.

In addition, SLAP primary transcript is also alternatively spliced in the 3' end of the SLAP gene common to all SLAP isoforms. Alternative splicing of the exon IV results

in an addition of a putative CKII phosphorylation consensus site and a predicted extension of the alpha-helical structure by 11 turns. The alternative exon X, on the other hand, encodes a highly hydrophobic segment containing an in-frame stop codon at the 3' terminal of the exon. Exon X, therefore could perhaps represent an alternative C-terminus encoding a novel transmembrane domain. Although functional evidence is lacking, the conservation of alternative splicing of: (1) the 51 and the 63 nt exons in rabbit and human, (2) exon IV in rabbit, rat and chick and (3) exon X in rabbit, human and chick strongly suggests that alternative variants may have distinct functional roles, as the alternative splicing has been maintained during evolution by natural selection.

An analysis of the alternatively spliced variants of SLAP revealed developmental changes in the expression of the 5' alternative variant in rat brain, kidney, lungs and spleen. In addition expression of the alternative variants was shown to be tissue-specific. The 51 and the 63 nt putative alternative exons, as well as the 5' (exon IV) and TM (exon X) alternative exons were expressed in all tissues, however in different amounts.

The observed developmental and tissue-specific splicing of the alternative exons is indicative of a functional differentiation of the alternative variants. Conversely in absence of a functional differentiation the natural selection would have eliminated the alternatively spliced variants. Interestingly, SLAP heterogeneity due to alternative N-terminal usage and diversity due to alternative splicing could together generate 36 distinct SLAP variants. The exact effect of SLAP variant heterogeneity on its function, subcellular localization, or intermolecular interactions remains unclear, and further work is required to characterize a role of individual alternative regions, alone and in combination.

The alternative splicing represents a fundamental process that generates tissue-specific and developmentally regulated pattern of gene expression. Many cardiac genes are alternatively spliced eg; (1) L-type Ca^{2+} channel responsible for 'trigger' Ca^{2+} undergoes alternative splicing that parallels major changes in myocyte excitation occurring during development (Diebold 1992). (2) Troponin-T, responsible for the coupling of the troponin complex to tropomyosin, is also spliced in a tissue and developmentally specific pattern, that correlates with myofilament sensitivity changes to Ca^{2+} (Townsend 1995 and Jin 1992). (3) Tropomyosin gene (TM-4) is alternatively spliced to yield cardiac and non-muscle specific isoforms (Hardy 1995).

Although the mechanism regulating the alternative splicing of SLAP alternative exons has not yet been studied, it might perhaps be regulated by splicing factors interacting with sequence elements in the adjacent introns, similar to beta-tropomyosin (Tsukahara 1994). At present, however, little is known about cellular factors and specific mechanisms that are responsible for cardiac specific alternative splicing and how they differ from processing of constitutive exons.

This study also shows, that there exist species specific differences in the expression of exon IV variants in adult rat and rabbit heart. Although, rat myocardium appears to express only a SLAP variant without the alternative exon IV, rabbit on the other hand also expresses a variant containing the alternative exon IV. Although there are reported differences in the Ca^{2+} homeostasis during E-C coupling between rabbit and rat ventricular myocytes (Rich 1988), it is unknown whether species-specific expression of SLAP variants could account for the observed differences.

It is well documented that protein components of the myocardial membranes play a pivotal role in E-C coupling, in signal transduction and regulation of ion fluxes. Although DHP and RYR receptors have been unequivocally identified as the functional determinants of E-C coupling, ablation of the 'foot' structures, RYR1 receptors, resulted in the absence of E-C coupling in homozygous offsprings of transgenic mice. Interestingly, however the junctions between surface membrane/t-tubules and SR were still formed (Takekura 1995). The formation of junctional couplings, therefore, appears to be mediated by additional proteins independently of RYRs and DHP receptors. These proteins, in addition may perhaps also play a role in spatial organization of DHPs and RYRs in the junctional couplings.

Northern Blot analysis revealed high level of expression of SLAP1 and SLAP2 isoforms in heart and slow-twitch muscle, but not fast-twitch muscle. Moreover previous immuno-histochemical studies demonstrated subcellular localization of SLAP in sarcolemma, T-tubules and sarcoplasmic reticulum. The level and muscle specific expression of SLAPs and their localization strongly suggests an important role in the function of a cardiomyocyte. Localization of SLAPs on both plasma membrane/T-tubules and SR membranes makes SLAP a good candidate for protein-protein interactions of the E-C coupling apparatus.

SLAP appears to be related to a new emerging family of tail-anchored proteins, that lack a signal sequence and contain a single hydrophobic segment at the C-terminus, leaving most of the polypeptide chain in the cytoplasm. Several members of the tail-anchored family of proteins are involved in cellular processes including: docking and fusion of

synaptic vesicles with plasma membrane (syntaxin and synaptobrevin) and vesicle trafficking.

SLAP is structurally similar to the syntaxin family, with a C-terminal membrane anchor domain and an extended alpha-helical structure, however does not share significant sequence similarity with syntaxins. Syntaxin family is constituted by at least six syntaxins that act as target membrane specific receptors in vesicle transport pathway. Syntaxin 5, and its yeast homologue SED5, for example are localized to either the Golgi complex or an ER-Golgi intermediate compartment. Syntaxins 1A/1B are localized to plasma membrane and are involved in docking and/or fusion reaction between neurotransmitter containing vesicle and the plasma membrane. Syntaxins 2 and 4 are also found in plasma membrane, suggesting that plasma membrane is a fusion partner for several different classes of transport vesicles.

Despite structural conservation of the syntaxin family, the individual family members do not share common sequence motifs, as those found in multigene families. It has been postulated that syntaxin family proteins form intermolecular coiled-coil structures with other protein components of the vesicular transport pathway machinery, and thus mediate vesicle targeting, membrane fusion and endocytotic membrane recycling. Syntaxin 1 is a neuronal cell membrane protein, that via its coiled-coil motifs interacts with SNAP-25 (Zhang 1997), synaptobrevin (Chapman 1994) and indirectly with synaptotagmin, a Ca^{2+}-sensor of vesicle endocytosis. In addition, syntaxin also interacts with N-type Ca^{2+} channel (Sheng 1996), thus localizing it to the site of vesicle release. The direct binding between components of exocytotic machinery is mediated by alpha-

helical heptad domains that form intermolecular coiled-coil structures.

SLAP protein, which is structurally similar to syntaxin family, contains an extended alpha-helical structure predicted to form coiled-coils over most of its length which would allow for many potential protein-protein interactions. SLAP protein localized to plasma membrane\T-tubules and SR membrane, might be an important player in the E-C coupling junctions, perhaps providing a structural manifold for establishment of coupling junctions between the cell membrane and SR. These interaction might be perhaps mediated by direct homophilic protein-protein interactions between SLAPs expressed in the cell membrane/t-tubules and SR, or by heterophilic associations with other protein partners of junctional couplings (Figure 15). The putative interactions between SLAPs might be mediated by formation of intermolecular coiled-coil structures over most of SLAP length or by the coiled-coil association of the leucine zipper. The coiled-coil associations have been demonstrated in many muscle proteins such as tropomyosin (Kohn 1997), where in each heptad, positions **a** and **d** are usually occupied by hydrophilic residues rendering amphipathic nature to the alpha helix (Adamson 1993). Hydrophobic face was also shown to play a role in transcription factor dimerization (Landschulz 1988 and Lehrer 1991). In addition SLAP contains seven glutamates in a row at the **g** position of the leucine zipper region giving a negatively charged region to the helix. Acidic amphipathic alpha-helices have been implicated to play a role in transcription potential of various transcription factors (Hollenberg 1988 and Cress 1991). Although a role of the glutamate zipper motif in SLAP is unclear, it may perhaps function to determine specificity of protein-protein interactions by modulating interactions between SLAPs

Figure 15. Hypothetical Role of SLAP in Junctional Couplings and Comparison with Syntaxin in excitation-secretion coupling.

Panel A depicts a schematic diagram of the exocytotic membrane fusion machinery involved in excitation-secretion coupling. Syntaxin is a presynaptic membrane protein that interacts with synaptobrevin and SNAP-25 to dock synaptic vesicle at the presynaptic membrane or to form an activated, fusion-ready vesicle (Sollner 1993 and Pevsner 1994). In addition, syntaxin also interacts with N-type Ca^{2+} channel thus localizing it to the site of vesicle release (Sheng 1996), as well as synaptotagmin, a Ca^{2+} sensor of the vesicle exocytosis. The multimeric protein complex is firmed via intermolecular protein-protein interactions occurring through the adaptation of the coiled-coil structures. Panel B depicts a schematic model of a junctional coupling. SLAP protein which is structurally similar to syntaxin is postulated to dock sarcoplasmic reticulum to cell membrane/T-tubules. SLAPs being located in both the sarcolemmal and SR membranes might perhaps via homophilic associations and/or heterophilic interactions with other protein partners couple these two membranes systems. Such structural coupling complex is perhaps formed and/or regulated by adaptation of coiled-coil structure, dimerization of leucine zippers and/or by interaction of negatively charged glutamate stretch with positively charged molecules. Alternative transmembrane domains of SLAP might direct SLAP isoforms to distinct target membranes.

A)

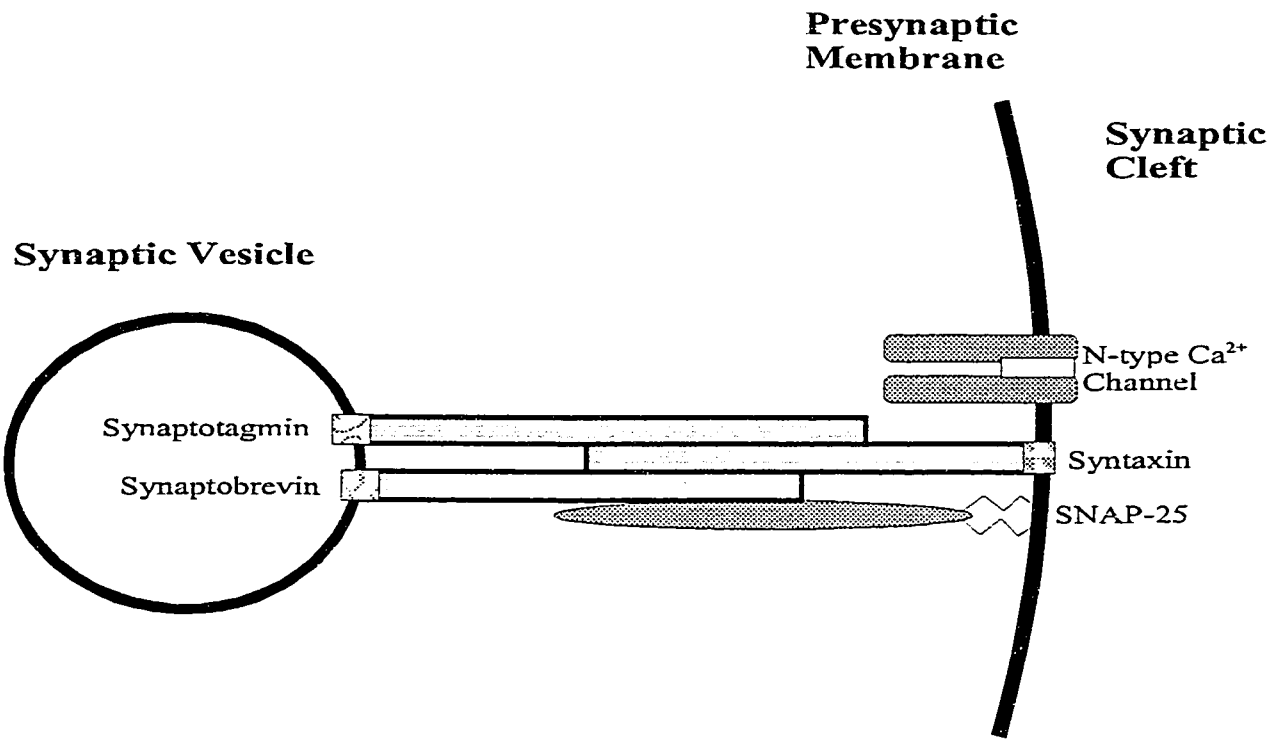
Presynaptic Membrane
Synaptic Cleft
Synaptic Vesicle
N-type Ca^{2+} Channel
Synaptotagmin
Synaptobrevin
Syntaxin
SNAP-25

B)

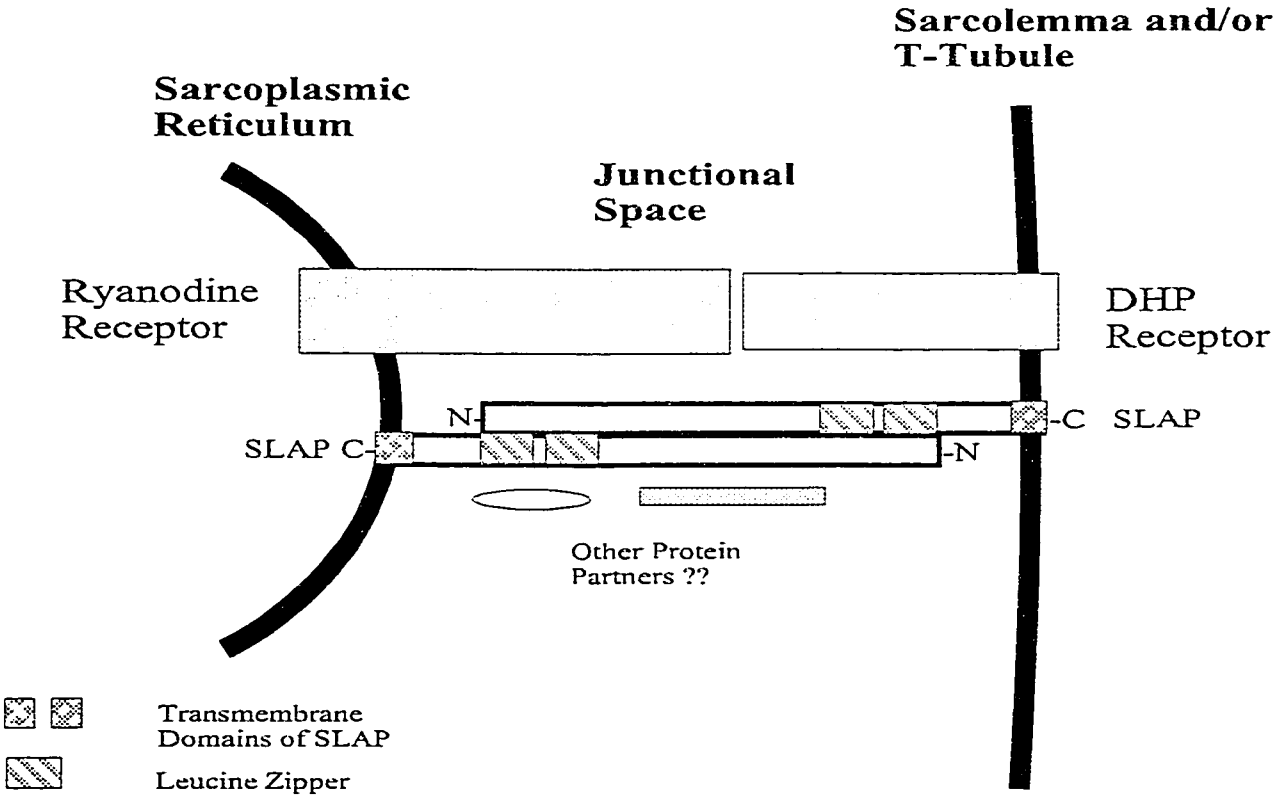
Sarcolemma and/or T-Tubule
Sarcoplasmic Reticulum
Junctional Space
Ryanodine Receptor
DHP Receptor
N-
-C SLAP
SLAP C-
-N
Other Protein Partners ??
Transmembrane Domains of SLAP
Leucine Zipper

and/or other protein partners, as well as with positively charged molecules and perhaps Ca^{2+} ions. Although, the exact role of the leucine and glutamate domains remains to be established, they are suggestive of further functional complexity to the SLAP protein.

Syntaxin 2 is the only tail-anchored family member known to contain alternative transmembrane domains, similar to SLAP protein described herein (Bennett 1993). The carboxyl-terminal of syntaxin-2 diverges after amino acid 264 to generate three alternative carboxyl-terminal sequences; two of which are of equal length and hydrophobicity (2 and 2'), and the third (2'') a 10 aa sequence including only six hydrophobic residues. Syntaxin 2 and 2' C-terminal ends are predicted to form transmembrane anchors while the 2'' end, although not of sufficient length or hydrophobicity to span the membrane, it could potentially be post-translationally modified by a lipid moiety to allow membrane anchoring. In view of the fact that syntaxin generates different carboxyl termini by alternative splicing, a specific function for the variants beyond simply anchorage of syntaxin to the membrane is suggested.

Similarly, alternative splicing of the mutually exclusive carboxyl-terminal transmembrane domains of SLAP suggests a functional specialization beyond simply anchoring to the membrane. In light of immunohistochemical localization to plasma membrane/t-tubules and SR membrane, perhaps the hydrophobic carboxyl terminals are involved in directing SLAP localization to specific target membranes or to specific domains of the plasma or SR membrane. Further immunohistological studies with cell lines stably expressing SLAP variants with mutually exclusive TM anchors are, however required to address the hypothesis of differential membrane targeting by the mutually

exclusive alternative transmembrane domains of SLAP.

A sequence homology search of genebank using BLAST algorithm identified a 73% aa identity between SLAP1 and a chick retinal cDNA, called TOP_{AP}. TOP_{AP} is believed to be an antigen involved in neuronal guidance in the retino-tectal pathway. Interestingly, however deduced secondary structures of TOP_{AP} and SLAP1 are similar, sharing the C-terminal transmembrane domain, predicted coiled-coil structure, leucine zippers and a negative glutamate stretch. In addition, the SLAP alternative exons (exons IV and X) are also found in TOP_{AP} cDNA sequence. The length of the SLAP alternative exons and their sites of insertion are identical in the chick retinal TOP_{AP}. Furthermore, the chick retinal TOP_{AP}-like variants containing the alternative exons IV and X were also identified in rabbit heart, rat retina and human heart orthologues of SLAP. In light of all the aforementioned evidence, the chick retinal TOP_{AP}, therefore represents an avian orthologue of mammalian SLAPs (rabbit, human, rat and mouse), where mammalian and avian orthologues originated from a common ancestral gene preceding a mammalian-avian lineage divergence.

Although, TOP_{AP} was postulated to play a role in establishing topographically specific retinotectal synaptic connections (Savitt 1995), SLAP1 was instead shown to accumulate at the contact interface between the adjacent cells membranes as well as to localize to intracellular membrane compartments (Wigle 1997). In addition, SLAP expression was highly localized in Mueller glial cells and was not detectable in retinal ganglion cells nor the optic nerve in contrast to expression of TOP_{AP} reported in both glia and neurons (Savitt 1995). The original immunohistologhical characterization of the

TOP_{AP} antigen in chick retinotectal pathway was performed with a monoclonal antibody that was subsequently used to isolate and characterize TOP_{AP} cDNA from chick retinal expression library. However, the immunohistochemical results were not presented using antibodies raised against isolated TOP_{AP} polypeptide. Moreover, TOP_{AP} mRNA levels in retinotectal system did not correlate with the observed topographical gradient of TOP_{AP} antigen. It is conceivable that the monoclonal antibody recognized an epitope of TOP_{AP} antigen and that the isolated cDNA does not truly represent topographically graded antigen of the retinotectal pathway. As SLAP expression is detectable in retinal glial cells, and not neurons, it is therefore unlikely that SLAP plays a role of a position antigen in the developing mammalian visual system. Further more SLAP topology is inconsistent with its role of an extracellular position marker as SLAP was shown to be an integral protein oriented cytoplasmically.

In summary, this study demonstrated that SLAP diversity is generated by alternative splicing, that in conjunction with the N-terminal heterogeneity could potentially generate more that 36 distinct SLAP variants. The alternatively spliced exons were shown to be conserved among mammalian and avian species, indicating that mammalian and avian orthologues originated from a common ancestral gene. Furthermore, the study elucidated the genomic organization of the 3' end of the SLAP gene.

REFERENCES

Adamson, J.G., Zhou, N.E. and R.S. Hodges. 1993. Structure, function and application of the coiled-coil protein folding motif. *Curr. Opin. Biotechnol.* **4**: 428-437.

Allende, J.E. and C.C. Allende. 1995. Protein kinases. Protein kinase CK2: an enzyme with multiple substrates and a puzzling regulation. *FASEB J.* **9**: 313-323.

Altschul, S.F., W. Gish, W. Miller, E.W. Myers and D.J. Lipman. 1990. Basic local alignment search tool. *J Mol Biol.* **215**:403-410.

Appel, R.D., A. Bairoch and D.F. Hochstrasser. 1994. A new generation of information retrieval tools for biologists: The example of the ExPASy WWW server. *Trends Biochem. Sci.* **19**: 258-260.

Arai, M., H. Matsui and M. Periasamy. 1994. Sarcoplasmic reticulum gene expression in cardiac hypertrophy and heart failure. *Circ. Res.* **74**:555-4564.

Au, K.S. 1986. Activation of erythrocyte membrane Ca2+-ATPase by calpain. *Biochim. Biophys. Acta* **905**: 273-278.

Ausubel, F., R. Brent, R.E. Kingston, D.D. Moore, J.G. Seidman, J.A. Smith and K. Struhl. 1995. Current Protocols in Molecular Biology, *John Willey & Sons*

Bean, B.P. 1985. Two kinds of calcium channels in canine atrial sells. Differences in kinetics, selectivity and pharmacology. *J. Gen. Physiol.* **86**: 1-30.

Bennett, M.K., J.E. Garcia-Arraras, L.A. Elferiuk, K. Peterson, A.M. Fleming, C.D. Hazuka and R.H. Scheller. 1993. The syntaxin family of the vesicular transport receptors. *Cell* **74**: 863-873.

Bers, D.M. and G.A. Langer. 1979. Uncoupling cation effect on cardiac and sarcolemmal Ca^{2+} binding. *Am. J. Physiol.* **237**: H332-H341.

Bers, D.M., J.W.M. Bassani and R.A. Bassani. 1993. Competition and redistribution among calcium transport systems in rabbit cardiac myocytes. *Cardiovasc. Res.* **27**:1772-1777.

Berridge, M. J. 1993. Inositol triphosphate and calcium signaling. *Nature* **361**: 315-325.

Birnboim, H.C. and J. Doly. 1979. A rapid alkaline extraction for screening recombinant plasmid DNA. *Nucl. Acids Res* **7**: 1513-1522.

Bouchard, R.A., R.B. Clark and W.R. Giles. 1995. Effects of action potential duration on excitation-contraction coupling in rat ventricular myocytes. Action potential voltage-clump measurements. *Circ. Res.* **76**:790-801.

Brandl, C.J., N.M. Green, B. Korczak, and D.H. MacLennan. 1986. Two Ca2+ ATPase genes: homologies and mechanistic implications of deduced amino acid sequences. *Cell* **44**:597-607.

Brandt, P., E. Ibrakin, G.A.P. Burns and R.L. Neve. 1992. Determination of the nucleotide sequence and chomosomal localization of the APTB2 gene encoding human Ca2+ pumping ATPase isoform PMCA2. *Genomics* **14**:484-487.

Brown, B.J., H. Hilfiker, S.J. DeMarko, D.A. Zacharias, T.M. Greenwood, D. Guerini and E.E. Strehler. 1996. Primary structure of human plasma membrane Ca(2+)-ATPase isofrom 3. *Biochim Biophys Acta* **1283**: 10-13.

Burk, S., J. Lytton, D.H. MacLennan and G. Shull. 1989. cDNA cloning, functional expression, and mRNA distribution of a third organellar Ca^{2+}-pump. *J. Biol. Chem.* **264**:18561-18568.

Cannell, M.B., H. Cheng and W.J. Lederrer W.J. 1994. Spacial non-uniformities in [Ca2+]i during excitation-contraction coupling in cardiac myocytes. *Biophysical J.* **67**: 1942-1956.

Cannell, M.B., H. Cheng and W.J. Lederer. 1995. The control of calcium release in heart muscle. *Science.* **268**:1045-1049.

Carifoli, E. 1985. The homeostasis of calcium in heart cells. *J. Mol. Cell Cardiol.* **17**:203-212.

Carafoli, E. 1987. Intracellular calcium homeostasis. *Ann. Rev. Biochem.* **56**:395-433.

Carafoli, E., F. Kessler, R. Falchetto et al. 1992. The molecular basis of the modulation of the plasma membrane calcium pump by calmodulin. *Ann. NY Acad.* Aci. **671**:58-69.

Caroni, P. and E. Carafoli. 1981. Regulation of the Ca2+ pumping ATPase of the heart sarcolemma by phosphorylation-dephosphorylation process. *J. Biol. Chem.* **256**:9371-9373.

Caroni, P. and E. Carafoli. 1983. The regulation of the Na+-Ca2+ exchange of heart sarcolemma. *Eur. J. Biochem.* **132**: 451-460.

Castellano, A. and E. Perez-Reyes. 1994. Molecular diversity of calcium channel beta subunits. *Biochem Soc Trans* **22**:483-488.

Caswell, A.H. and N.R. Brandt. 1989. Does muscle activation accur by direct mechanical coupling of transverse tubules to sarcoplasmic reticulum. *Trends Biochem. Sci.* **14**: 161-165.

Catterall, W.A. 1988. Structure and function of voltage-sensitive channels. *Science.* **242**:50-61.

Catterall, W.A. 1991. Excitation-Contraction coupling in vertebrate skeletal muscle: a tale of two calcium channels. *Cell.* **64**:871-874.

Catterall, W.A. and J. Striessnig. 1992. Receptor sites for calcium antagonists. *Trends Pharmacol Sci.* **13**:256-262.

Catterall, W.A. 1993. Structure and function of voltage-gated ion channels. *Trends Neurosci.* **16**: 500-506.

Chadwick, C.C., A. Saito and S. Fleischer. 1990. Isolation and characterization of the inositol triphosphate receptor from smooth muscle. *Proc. Natl. Acad. Sci. U.S.A.* **87**: 2132-2136.

Chapman, E.R., S. An, H. Barton and R. Jahn. 1994. SNAP-25, a t-SNARE which binds to both syntaxin and synaptobrevin via domains that may form coiled coils. *J. Biol. Chem.* **269**: 27427-27432.

Chomczynski, P. 1993. A reagent for the single-step simultaneous isolation of RNA, DNA and protein from cell and tissue samples. *Biotechniques* **15**: 532-537.

Cress, W.D. and S.J. Triezenberg. 1991. Critical elements of the VP16 transcriptional activation domain. *Science* **251**: 87-90.

Demchyshyn, L.L. 1990. Isolation of complementary DNA for heart sarcolemmal antigens. M.Sc. Thesis. University of Toronto.

Diebold, R.J., W.J. Koch, P.T. Ellinor, J.J. Wang, M. Muthuchammy, D.F. Wieczorek and A. Schwartz. 1992. Mutually exclusive exon splicing of the cardiac calcium channel alpha 1 subunit gene generates developmentally regulated isoform in the rat heart. *Proc. Natl. Acad. Sci. USA.* **89**: 1497-1501.

Ebashi, S. 1976. Excitation-Contraction Coupling. *Ann. Rev. Physiol.* **38**:293-313.

Fabiato, A. 1983 Calcium-induced release of calcium from the cardiac sarcoplasmic reticulum. *Am. J. Physiol.* **245**:c1-c14.

Fabiato, A. 1985. Time and calcium dependent activation and inactivation of calcium-induced release of calcium from the sarcoplasmic reticulum of a skinned cardiac Purkinje cell. *J. Gen. Physiol.* **85**: 247-289.

Feher, J.J., F.N. Briggs and M.L. Hess. 1980. Characterization of cardiac sarcoplasmic reticulum from ischemic myocardium: comparison of isolated sarcoplasmic reticulum with unfractioned homogenates. *J. Mol. Cell. Cardiol.* **12**: 427-432.

Fleischer, S and M. Inui. 1989. Biochemistry and biophysics of excitation-contraction coupling. *Ann. Rev. Biophys. Chem.* **18**: 333-364.

Fliegel, L., M. Ohnishi, M.R. Carpenter, V.K. Khanna, R.A.F. Reithmeier and D.M. MacLennan. 1987. Amino acid sequence of rabbit fast-twitch skeletal muscle calsequestrin deduced from cDNA and peptide sequencing. *Proc. Natl. Acad. Sci. U.S.A.* **84**: 1167-1171.

Fliegel, L., E. Leberer, N.M. Green, and MacLennan. 1989a. The fast-twitch muscle calsequestrin isoform predominates in rabbit slow-twitch soleus muscle. *FEBS Lett.* **242**: 297-300.

Fliegel, L., K. Burns, D.H. MacLennan, R.A.F. Reithmeier and M. Michalak. 1989b. Molecular cloning of the high affinity calcium-binding protein (calreticulin) of skeletal muscle sarcoplasmic reticulum. *J. Biol. Chem.* **264**: 21522-21528.

Flucher, B.E. and C. Franzini-Armstrong. 1996. Formation of junctions involved in the excitation-contraction coupling in skeletal and cardiac muscle. *Proc. Natl. Acad. Sci. USA.* **93**: 8101-8106.

Franzini-Armstrong, C. and A.O. Jorgensen. 1994. Structure and development of excitation-contraction coupling units in skeletal muscle. *Annu. Rev. Physiol.* :509-534.

Fujii, J., A. Zarain-Herzberg, H.F. Willard, M. Tada and D.M. MacLennan. 1991. Structure of the rabbit phospholamban gene, cloning of the human cDNA, and assignment of the gene to human chromosome 6. *J. Biol. Chem.* **266** :11669-11675.

Gasser, J., P. Paganetti, E. Carafoli and M. Chiesi. 1988. Heterogenous distribution of calmodulin- and cAMP-dependent regulation of Ca2+ uptake in cardiac sarcoplasmic

reticulum subfractions. *Eur. J. Biochem.* **176**: 535-541.

Guo, W., A.O. Jorgensen, L.R. Jones and K.P. Campbell. 1996. Biochemical localization and molecular cloning of cardiac triadin. *J. Biol. Chem.* **271**: 458-465.

Hardy, S., N. Theze, D. Lepetit, M.R. Allo and P. Thiebaud. 1995. The Xenopus laevis TM-4 gene encodes non-muscle and cardiac tropomyosin isoforms through alternative splicing. *Gene.* **156**: 265-270.

Heim, R., M. Hug, T. Iwata, E.E. Strehler and E. Carafoli. 1992. Microdiversity of the human-plasma-membrane calcium-pump isoform 2 generated by alternative RNA splicing in the N-terminal coding region. *Eur. J. Biochem.* **205**: 333-340.

Hofmann, S.L., M.S. Brown, E. Lee, R.K. Pathak, R.G.W. Anderson, and J.L. Goldstein. 1989a. Purification of a sarcoplasmic reticulum protein that binds Ca2+ and plasma lipoproteins. *J. Biol. Chem.* **264**: 8260-8270.

Hofmann, S.L., J.L. Goldstein, K. Orth, C.R. Moomaw, C.A. Slaughter and M.S. Brown. 1989b. Molecular cloning of a histidine-rich Ca2+-binding protein of sarcoplasmic reticulum that contains highly conserved repeated elements. *J. Biol. Chem.* **264**: 18083-18090.

Hollenberg, S.M. and R.M. Evans. 1988. Multiple and cooperative transactivation domain of the human glucocorticoid receptor. *Cell* **55**: 899-906.

Huxley, A.F. Muscle structure and theories of contraction. 1957. *Prog. Biophys. Chem.* **7**: 255-318.

Jan, L.Y., and Y.N. Jan. 1989. Voltage-sensitive ion channels. *Cell* **56**: 13-25.

Jin, J.P., Q.Q. Huang, H.I. Yeh and J.J. Lin. 1992. Complete nucleotide sequence and structural organization of rat cardiac troponin T gene. A single gene generates embryonic

and adult isoforms via developmentally regulated alternative splicing. *J. Molec. Biol.* **227**: 1269-1276.

Jones, L.R., L. Zhang, K. Sanborn, A.O. Jorgensen and J. Kelley. 1995. Purification, primary structure, and immunological characterization of the 26-kDa calsequestrin binding protein (junctin) from cardiac junctional sarcoplasmic reticulum. *J. Biol. Chem.* **270**: 30787-30796.

Jorgensen, A.O. and L.R. Jones. 1987. Immunoelectron microscopical localization of phospholamban in adult canine ventricular muscle. *J. Cell Biol.* **104**: 1343-1352.

Kofuji, P., W.J. Lederer and D.M. Schulze. 1994. Mutually exclusive and cassette exons underlie alternatively spliced isoform of the Na/Ca exchanger. *J. Biol. Chem.* **269**: 5145-5149.

Kohn, W.D., Mant, C.T. and R.S. Hodges. 1997. Alpha-helical protein assembly motif. *J. Biol. Chem.* **272**: 2582-2586.

Kohomoto, O., A.J. Levi and J.H. Bridge. 1994. Relation between reverse sodium-calcium exchange and sarcoplasmic reticulum calcium release in guinea pig ventricular cells. *Circ. Res.* **74**: 550-554.

Kosk-Kosicka, D. and T. Bzdega. 1988. Activation of the erythrocyte Ca2+-ATPase by either self-association or interaction with calmodulin. *J. Biol. Chem.* **263**: 18184-18189.

Kostyuk, P.G. 1989. Diversity of Calcium Ion Channels in Cellular Membranes. *Neuroscience* **28**: 253-261.

Kretsinger, R.H. and C.E. Knockolds. 1973. Carp muscle calcium-binding protein. II Structure determination and general description. *J. Biol. Chem.* **248**: 3313-3326.

Krogh, A., M. Browm, I.S. Miam, K. Sjolander and D. Haussler. 1994. Hidden Markov models in computational biology. Applications to protein modeling. *J. Mol. Biol.* **235**:

1501-1531.

Landschulz, W.H., P.F. Johnson and S.L. McKnight. 1988. The leucine zipper: A hypothetical structure common to a new class of DNA binding proteins. *Science.* **240**: 1759-1764.

Langer, G.A. and L.M. Nudd. 1983. Effects of Cations, phospholipases and neuraminidase on calcium binding to "gas-dissected" membranes from cultured cardiac cells. *Circ. Res* **53**: 482-490.

Leberer, E., J.H.M. Charuk, D.M. Clarke, N.M. Green and D.H. MacLennan. 1989a. Molecular cloning and expression of cDNA encoding a lumenal calcium binding glycoprotein from sarcoplasmic reticulum. *Proc. Natl. Acad. Sci. U.S.A.* **86**: 6047-6051.

Leberer, E., J.H.M Charuk,D.M. Clarke, N.M. Green, E. Zubrzycka-Gaarn and D.H. MacLennan. 1989b. Molecular cloning and expression of cDNA encoding the 53,000-Dalton glycoprotein of rabbit skeletal muscle sarcoplasmic reticulum. *J. Biol. Chem.* **264**: 3484-3493.

Leberer, E., B.G. Timms, K.P. Campbell and D.H. MacLennan. 1990. Purification, calcium binding proteins, and ultrastructural localization of the 53,000 and 160,00 (sarcalumenin) Dalton glycoproteins of sarcoplasmic reticulum. *J. Biol. Chem.* **265**: 10118-10124.

Leblanc, N. and J.R. Hume. 1990. Sodium current-induced release of calcium from cardiac sarcoplasmic reticulum. *Science* **248**: 372-376.

Lehrer, S. and W. Stafford. 1991. Preferential assembly of the tropomyosin heterodimer: equilibrium studies. *Biochemistry* **30**: 5682-5688.

Levesque, P.C., N. Leblanc and J.R. Hume. 1991. Role of reverse-mode Na(+)-Ca2+ exchange in excitation-contraction coupling in the heart. *Ann. NY Acad. Sci.* **639**: 386-397.

Levi, A.J., P. Brooksby and J.C. Hancox. 1993. A role for depolarization induced calcium entry on the Na-Ca exchanger in triggering intracellular calcium release and contraction in rat ventricular myocytes. *Cardiovasc Res.* **27**: 1677-1690.

Litwin, S., O. Kohomoto, A.J. Levi, K.W. Spitzer and J.H. Bridge. 1996. Evidence that reverse Na^{+}-Ca^{2+} exchange can trigger SR calcium release. *Ann. NY Acad. Sci.* **779**: 451-463.

Lokuta, A.J., M.B. Meyers, P.R. Sanders, G.I. Fishman and H.H. Voldivia. 1997. Modulation of cardiac ryanodine by sorcin. *J. Biol. Chem.* **272**: 25333-25338.

Lupas, A., M. Van Dyke and J. Stock. 1991. Predicting coiled-coils from protein sequences. *Science.* **252**: 1162-1164.

Lytton, J. and D.H. MacLennan. 1988. Molecular cloning of cDNA from human kidney coding for two alternatively spliced products of cardiac Ca2+-ATPase gene. *J. Biol. Chem.* **263**: 15024-15031.

Lytton, J., A. Zarain-Herzberg, M. Periasamy and D.H. MacLennan. 1989. Molecular cloning of the mammalian smooth muscle sarco(endo)plasmic reticulum Ca2+-ATPase. *J. Biol. Chem.* **264**: 7059-7065.

Lytton, J. and D.H. MacLennan. 1992. Sarcoplasmic Reticulum. In Fozzard, H.A. *et al.* 2nd ed. New York, Raven Press. 1203-1222.

MacKenzie, A.E., R.G. Korneluk, F. Zorzato, J. Fujii, M. Philips, D. Iles, B. Wieringa, S. Leblond, J. Bailly, H.F. Willard, C. Duff, R.G. Warton and D.H. MacLennan. 1990. The human ryanodine receptor gene: its mapping to 19q13.1, placement in a chromosome linkage group, and exclusion as the gene causing myotonic dystrophy. *Am. J. Hum. Genet.* **46**: 1082-1089.

MacLennan, D.H., C.J. Brandl, B. Korczak and N.M. Green. 1985. Amino acid sequence of a Ca^{2+}-Mg^{2+}-dependent ATPase from rabbit muscle SR, deduced from its

complementary DNA structure. *Nature* **316**: 696-700.

MacLennan, D.H., C.J. Brandl, S. Champaneria, P.C. Holland, V.E. Powers and H.F. Willard. 1987. Fast-twitch and slow-twitch/cardiac Ca2+ ATPase genes map to human chromosomes 16 and 12. *Som. Cell Mol. Genet.* **13**: 341-346.

Matsuoka, S., D.A. Nicoll, Z. He, and K.D. Philipson. 1997. Regulation of cardiac Na(+)-Ca2+ exchanger by the endogenous XIP region. *J Gen Physiol* **109**: 273-286.

McLeod, A.G., A.C.Y. Shen, K.P. Campbell, M. Michalak and A.O. Jorgensen. 1991. Frog cardiac calsequestrin. Identification, characterization and subcellular distribution in two structurally distinct regions of peripheral sarcoplasmic reticulum in frog ventricular myocardium. *Circ. Res.* **69**: 344-359.

Meyers, M.B., V.M. Pickel, S.S. Sheu, V.K. Sharma, K.W. Scotto and G.I. Fishman. 1995. Association of sorcin with the cardiac ryanodine receptor. *J. Biol. Chem.* **270**: 26411-26418.

Mikami, A., K. Imoto, T. Tanaba, T. Niidome, Y. Mori, H. Takeshima, S. Narumiya and S. Numa. 1989. Primary structure and functional expression of the cardiac dihydropyridine calcium channel. *Nature* **340**: 230-233.

Mitcheson, J.S., J.C. Hancox and A.J. Levi. 1997. Voltage dependence of the Fura-2 transient in rabbit left atrial myocytes at 37 degrees C. *Pflugers Arch* **433**: 817-826.

Mount, S.M. 1982. A catalogue of splice junction sequences. *Nucleic Acids Res.* **10**: 459-472.

Nakai, J., B.A. Adams, K. Imoto and K.G. Beam. 1993. Critical roles of the S3 segment and S3-S4 linker of repeat I in activation of L-type calcium channels. *Proc. Natl. Acad. Sci. USA* **91**: 1014-1018.

Nicoll, D.A., S. Longoni and K.D. Philipson. 1990. Molecular cloning and function of

the cardiac sarcolemmal Na+-Ca2+ exchanger. *Science* **250**: 562-565.

Otsu, K., H.F. Willard, V.J. Khanna, F. Zorzato, N.M. Green and D.H. MacLennan. 1990. Molecular cloning of cDNA encoding the Ca2+ release channel (ryanodine receptor) of rabbit cardiac muscle sarcoplasmic reticulum. *J. Biol. Chem.* **265**: 13472-13483.

Pevsner, J., S.C. Hsu, J.E. Braun, N. Calakos, A.E. Ting, M.K. Bennett and R.H. Scheller. 1994. Specificity and regulation of a synaptic vesicle docking complex. *Nature* **13**: 353-361.

Philipson, K.D., Bers, D.M. and A.Y. Nishomoto. 1980. Role of the phospholipids in the Ca^{2+} binding of isolated sarcolemma. *J Mol Cell Cardiol* **12**: 1159-1173.

Rich, T.L., G.A. Langer and M.G. Klassen. 1988. Two components of coupling calcium in single ventricular cell of rabbit and rat. *Am J Physiol.* **254**: H937-H946.

Pinna, L.A. 1997. Protein kinase CK2. *Inter. J. Biochem. Cell. Biol.* **29**: 551- 554.

Rios, E., J. Ha and A. Gonzalez. 1991. The mechanical hypothesis of excitation-contraction coupling. *J. Muscle Res. Cell Motil.* **12**: 127-135.

Saito, A., M. Inui, M. Radermacher, J. Frank and S. Fleischer. 1988. Ultrastructure of the calcium release channel of sarcoplasmic reticulum. *J. Cell Biol.* **107**: 211-219.

Sambrook, J., E.F. Fritsch and T. Maniatis. 1989. Molecular cloning - A laboratory manual, 2nd Ed. Cold Spring Harbour Laboratory Press.

Sather, W.A., J. Yang and R.W. Tsien. 1994. Structural basis of ion channel permeation and selectivity. *Curr Opin Neurobiol* **4**: 313-323.

Savitt, J.M., D. Trisler and D.C. Hilt. 1995. Molecular Cloning of TOP_{AP}: A Topographically Graded Protein in the Developing Chick Visual System. *Neuron.* **14**: 253-

261.

Schwartz, A. 1989. Calcium antagonists: Review and perspective on mechanism of action. *Am. J. Cardiol.* **64**(Suppl.) 3I-9I.

Scott, B., H.K.B. Simmerman, J.H. Collins, B. Nadal-Ginard, and L.R. Jones. 1988. Complete amino acid sequence of canine cardiac calsequestrin deduced by cDNA cloning *J. Biol. Chem.* **263**: 8459-8964.

Sheng, Z.H., J. Rettig, T. Cook and W.A. Catterall. 1996. Calcium-dependent interaction of N-type calcium channels with the synaptic core complex. *Nature* **379**: 451-454.

Smith, M.J. and G.L.E. Koch. 1989. Multiple zones in the sequence of calreticulin (CRP 55, calregulin, HACBP) a major calcium binding ER/SR protein. *EMBO J.* **8**: 3581-3586.

Snutch, T.P. and P.B. Reiner. 1992. Ca2+ channels diversity of form and function. *Curr Opin Neurobiol* **2**: 247-253.

Soldatov, N.M. 1992. Molecular diversity of L-type Ca^{2+} channel transcripts in human fibroblasts. *Proc Natl Acad Sci USA.* **89**: 4628-4632.

Soldatov, N.M., A. Bouron and H. Reuter. 1995. Diferent voltage-dependent inhibition by dihydropyridines of human Ca^{2+} channels splice variants. *J. Biol. Chem.* **270**: 10540-10543.

Soldatov, N.M., R.D. Zuhlke, A. Bouron and H. Reuter. 1997. Molecular structures involved in L-type calcium channel inactivation. Role of the carboxyl-terminal region encoded by exons 40-42 in alpha1C subunit in the kinetics and Ca^{2+} dependence of inactivation. *J. Biol. Chem.* **272**: 3560-3566.

Sollner, T., S.W. Whiteheart, W. Brunner, H. Erdjument-Bromage, S. Geromanos, P. Tempst and J.E. Rothman. 1993. SNAP receptors implicated in vesicle targeting and fusion. *Nature* **362**: 318-324.

Stauffer, T.P., H. Hilfiker, E. Carafoli and E.E. Strehler. 1993. Quantitative analysis of the alternative splicing options of the human plasma membrane calcium pump. *J. Biol. Chem.* **268**: 25993-26003.

Stern, M.D. 1992. Theory of excitation-contraction coupling in cardiac muscle. *Biophysical J.* **63**: 497-517.

Strehler, E.E., P. James, R. Fisher, R. Heim, T. Vorherr, A.G. Filoteo, J.T. Penniston and E. Carafoli. 1990. Peptide sequence analysis and molecular cloning reveals two calcium ATPase isoforms in the human erythrocyte membrane. *J. Biol. Chem.* **265**: 2835-2842.

Takekura, H., M. Nishi, T. Noda, H. Takeshima and C. Franzini-Armstrong. 1995. Abnormal junctions between surface membrane and sarcoplasmic reticulum in skeletal muscle with a mutation targeted to the ryanodine receptor. *Proc. Natl. Acad. Sci. USA.* **92**: 3381-3385.

Takeshima, H., S. Nishimura, T. Matsumoto, H. Ishida, K., Kangawa, N. Minamino, H. Matsuo, M. Uedda, M. Hanaoka and T. Hirose. 1989. Primary structure and expression from complementary DNA of skeletal muscle ryanodine receptor. *Nature* **339**: 439-445.

Tanabe, T., K.G. Beam, J.A. Powell and S. Numa. 1988. Restoration of excitation-contraction coupling and slow calcium current in dysgenic muscle by dihydropyridine receptor complementary DNA. *Nature* **336**: 134-139.

Tanabe, T., A. Mikami, S. Numa, and K.G. Beam. 1990a. Cardiac-type excitation-contraction coupling in dysgenic skeletal muscle injected with cardiac dihydropyridine receptor cDNA. *Nature* **344**: 451-453.

Tanabe, T., K.G. Beam,B.A. Adams, T. Niidome and S. Numa. 1990b. Regions of the skeletal muscle dihydropyridine receptor critical for excitation-contraction coupling. *Nature* **356**: 567-569.

Tobacman, L.S. 1996. Thin filament-mediated regulation of cardiac contraction. *Annu. Rev. Physiol.* **58**: 447-481.

Toyoshima, C., H. Sasabe and D.L. Stokes. 1993. Three-dimensional cryo-electron microscopy of the calcium pump in the sarcoplasmic reticulum membrane. *Nature* **362**: 469-471.

Townsend, P.J., P.J. Barton, M.H. Yacoub and H. Farza. 1995. Molecular cloning of human cardiac troponin T isoform: expression in developing and failing heart. *J. Molec and Cell. Cardiology.* **27**: 2223-2236.

Tsien, R.W., P.T. Ellinor and W.A. Horne. 1991. Molecular diversity of voltage-dependent Ca^{2+} channels. *Trends Pharmacol Sci.* **12**: 349-354.

Tsukahara, T., C. Casciato and D.M. Helfman. 1994. Alternative splicing of beta-tropomyosin pre-mRNA: multiple cis-elements can contribute ti the use of the 5'- and 3'-splice sites of the nonmuscle/smooth muscle exon 6. *Nucleic Acids Res.* **22**: 2318-2325.

Tuana, B.S., A. Dzurba, V. Panagia and N.S. Dhalla. 1981. Stimulation of the heart sarcolemma calcium pump by calmodulin. *Biochem. Biophy. Res. Commun.* **100**: 1245-1250.

Tuana, B.S. and B.J. Murphy. 1990. Biochemical analysis of L-type calcium channels from skeletal and cardiac muscle. *Can. J. Physiol. Pharmacol.* **68**: 1482-1488.

Tuana, B.S., R.K. Sunahara, B.J. Murphy and G.N. Pierce. 1991. Two major antigens of heart sarcolemma are Ca+-binding glycoproteins that copurify with the dihydropyridine receptor. *Biochim Biophys Acta* **1091**: 236-241.

Varadi, G., Y. Mori, G. Mikala and A. Schwartz. 1995. Molecular determinants of Ca2+channel function and drug action. *Trends Pharmacol Sci.* **16**: 43-49.

Vassort, G. and J. Alvarez. 1994. Cardiac T-type calcium current: pharmacology and

roles in cardiac tissues. *J. Cardiovasc. Electrophysiol.* **5**: 376-393.

Verma, A.K., A.G. Filoleteo, D.R. Stanford, E.D. Wieben, J.T. Penniston, E.E. Strehler, R. Fisher, R. Heim, G. Vogel, S. Mathews, M-A. Strehler-Page, P. James, T. Vorherr, J. Krebs and E Carafoli. 1988. Complete primary structure of a human plasma membrane Ca2+ pump. *J. Biol. Chem.* **263**: 14152-14159.

Vogel, H.J. 1994. The Merck Frosst Award Lecture: Calmodulin, a versatile calcium mediator protein. *Biochem. Cell Biol.* **72**: 3571-3576.

Vogelstein, B. and D. Gillespie. 1979. Preparative and analytical purification of DNA from agarose. *Proc. Natl. Acad. Sci. USA.* **76**: 615-619.

Vorherr, T., T. Kessler, F. Hofmann and E. Carafoli. 1991. The calmodulin-binding domain mediates the self-association of the plasma membrane Ca2+ pump. *J. Biol. Chem.* **266**: 22-27.

Wagenknecht, T., R. Grassucci, J. Frank, A. Saito, M. Inui and S. Fleischer. 1989. Three-dimensional architecture of the calcium channel/foot structure of sarcoplasmic reticulum. *Nature* **338**: 167-170.

Wagenknecht, T. and M. Radermacher. 1997. Ryanodine receptors: structure and macromolecular interactions. *Curr Opin Struct Biol* **7**: 258-265.

Wang, K.K., A. Villalobo and B.D Roufogalis. 1988. Activation of the Ca2+-ATPase of the human erythrocyte membrane by an endogenous Ca2+-dependent neutral protease. *Arch. Biochem. Biophys. Acta.* **260**: 696-704.

Wang, K., L.C. Wright, C.L. Madian, B.G. Allen, A.D. Conigrave and B.D. Roufogalis. 1991. Protein kinase C phosphorylates the carboxyl terminus of the plasma membrane Ca2+-ATPase from the human erythrocytes. *J. Biol. Chem.* **266**: 9078-9085.

Wang, S.L., M.F. Tam, Y.S. Ho, S.H. Pai and M.C. Kao. 1995. Isolation and molecular cloning of human sorcin a calcium-binding protein in vincristine-resistant HOB1 lymphoma cells. *Biochim. Biophys. Acta* **1260**: 285-293.

Wibo, M., G. Bravo and T. Godraind. 1991. Postnatal maturation of excitation-contraction coupling in rat ventricle in relation to the subcellular location and surface density of 1,4-dihydropyridine and ryanodine receptors. *Circ. Res.* **68**: 662-673.

Wier, W.G., T.M. Egan, J.R.Lopez-Lopez and C.W. Balke. 1994. Local control of excitation-contraction coupling in rat heart cells. *J.Physiol.* **474**: 463-471.

Wigle, J., L. Demchyshyn, M.A.C. Pratt, W.A. Staines, M. Salih and B.S. Tuana. 1997. Molecular cloning, expression and chromosomal assignment of sarcolemma-associated proteins. *J. Biol. Chem.* **272**: 32384-32394.

Yamazawa, T., H. Takeshima, M. Shimuta and M. Iino. 1997. A region of the ryanodine receptor critical for the excitation-contraction coupling in skeletal muscle. *J. Biol. Chem.* **272**: 8161-8162.

Yoshida, Y., H-T. Sun, J-Q. Cai and S. Imai. 1991. Cyclic GMP dependent protein kinase stimulates the plasma membrane Ca2+ pump ATPase of vascular smooth muscle via phosphorylation of a 240-kDa protein. *J. Biol. Chem.* **266**: 19819-19825.

Zhang, P., Y.A. Chen, D. Tam, D. Chung and R.H. Scheller. 1997. An alpha-helical minimal binding domain within the H3 domain of syntaxin is required for SNAP-25 binding. *Biochemistry*. **36**: 4317-4326.

Zorzato, F., J. Fujii, K. Otsu, M. Philips, N.M. Green, F.A. Lai, G. Meissner and D.H. MacLennan. 1990. Molecular cloning of cDNA encoding human and rabbit forms of the Ca^{2+} release channel (ryanodine receptor) of skeletal muscle sarcoplasmic reticulum. *J. Biol. Chem.* **265**: 2244-2256.

IMAGE EVALUATION TEST TARGET (QA-3)

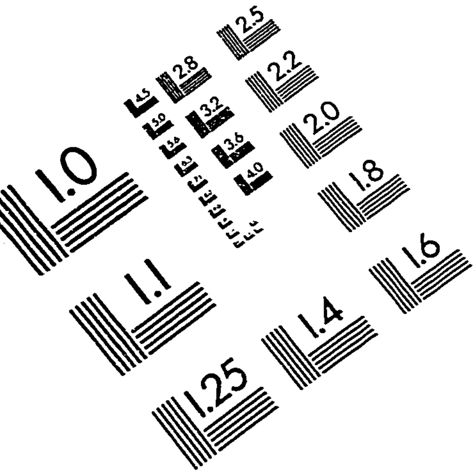

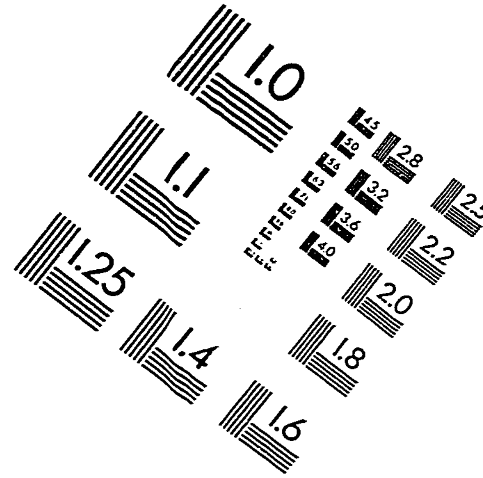

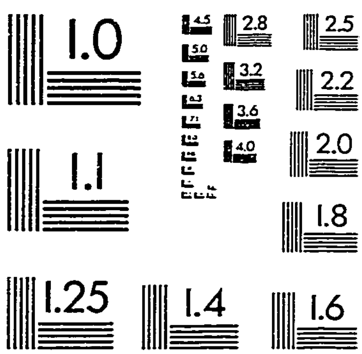

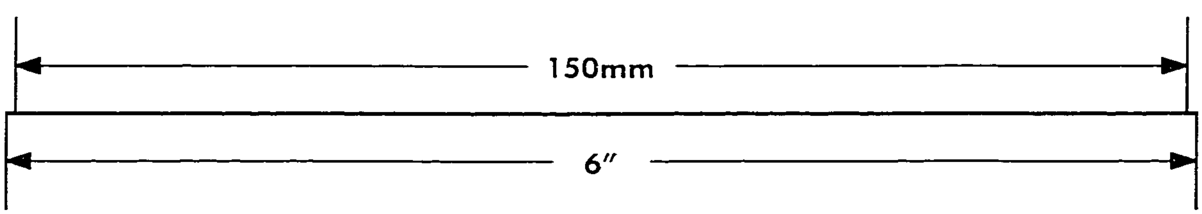

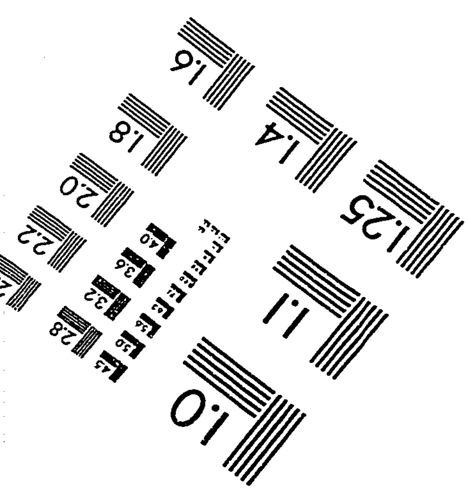

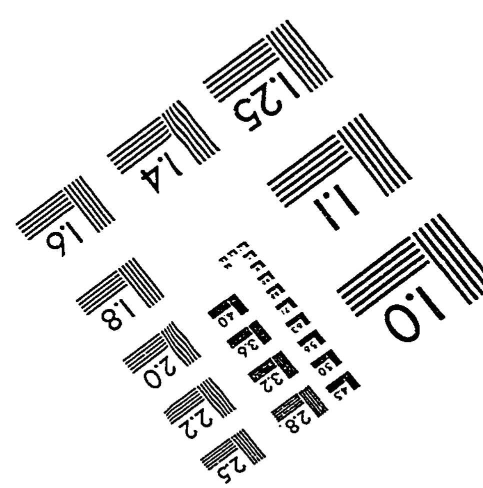

APPLIED IMAGE . Inc
1653 East Main Street
Rochester, NY 14609 USA
Phone: 716/482-0300
Fax: 716/288-5989